Exploring Cooperative NOMA Assisted Hybrid Visible Light and Radio Frequency for Enhanced Vehicular Message Dissemination at Road Intersections

Gurinder Singh[a], Dhanushi Gupta[a], Vivek Ashok Bohara[a], Anand Srivastava[a] and Zilong Liu[b]

[a]*Indraprastha Institute of Information Technology (IIIT)-Delhi, New Delhi, India-110020,*
[b]*School of Computer Science and Electronic Engineering, University of Essex, Colchester CO4 3SQ, U.K,*

ARTICLE INFO

ABSTRACT

Vehicle-to-everything (V2X) communication aims to achieve significantly improved safety and traffic efficiency, more particularly at road intersection where high percentage of accidents usually occur. The existing vehicular radio frequency (V-RF) based V2X utilizes relaying for improving safety message dissemination at road intersections. For a high traffic density scenario, the V-RF communication with relaying solution may suffer from large latency and low packet delivery rates due to channel congestion. In this paper, we explore cooperative non-orthogonal multiple access (NOMA) communication assisted hybrid vehicular visible light communication (V-VLC) and V-RF communication for improving safety message dissemination and enabling massive connectivity among vehicles for road intersection scenarios. We develop a stochastic geometry based analytical framework to model cooperative NOMA (C-NOMA) transmissions subject to interference imposed by other vehicles on roads. We also examine the impact of vehicles headlights radiation pattern viz. Lambertian and empirical path loss models on statistical characterization of the proposed C-NOMA supported hybrid solution. Our numerical findings reveal that C-NOMA assisted hybrid V-VLC/V-RF system leads to considerable improvement in outage performance and average achievable rate as compared to traditional V-RF solution with relaying. Interestingly, Lambertian model offers a lower outage and higher average achievable rate compared to the empirical model for the proposed hybrid solution. Further, we observe the performance improvement using maximal ratio combining (MRC) considering NOMA transmission for the proposed hybrid solution. The presented framework may serve as an alternative for cooperative intelligent transportation system (C-ITS) to meet diverse application needs for beyond 5G (B5G) V2X networks.

1. Introduction

According to world health organisation (WHO) survey statistics, approximately 1.3 million people died in 2021 as a result of road traffic crashes, more often at road intersections [1]. To improve the driving safety, intelligent transportation system (ITS) mechanisms are employed to provide efficient vehicle-to-vehicle (V2V) communications [2]. Presently, the information exchanges among moving vehicles and road infrastructure (e.g., traffic lights, lamp posts, etc) mostly rely on vehicular radio frequency (V-RF) communication. The traditional V-RF technology provides a long communication range and can pass through objects with tolerable degradation in performance. With the ever-growing data services and applications, however, the RF spectrum (especially the sub-6 GHz band) is becoming increasingly scarce and congested. Moreover, the effect of interference in a dense vehicular traffic scenario, as well as the resultant higher latency and reduced packet delivery rates when hundreds of vehicles communicate concurrently, are hindering the large scale development of V-RF based technology.

Vehicular visible light communication (V-VLC) has emerged as a promising complementary solution to the conventional V-RF. By employing light-emitting diodes (LEDs) as transmitters and photodiodes as receivers [3], V-VLC owns the potential of utilizing the existing lighting infrastructure to reduce fatal accidents. Due to the directional property of V-VLC, lower amount of interference is expected [4]. Further, its inherent features such as higher security, reduced cost of transceiver design, enhanced connectivity and less power consumption have made V-VLC one of the most promising candidate technologies for V2X communication. However, V-VLC becomes inept as the distance between the communicating vehicles increases, resulting in a limited communication coverage [5]. Further, V-VLC also requires line-of-sight (LOS) propagation which may be unavailable in outdoor surroundings, due to vehicular mobility and environmental effects in different geolocations and weather conditions. Thus, it is necessary to integrate V-RF and V-VLC to deliver enhanced vehicular safety message dissemination. On one hand, V-VLC aims for achieving higher data rates and reduced interference for each communication link. On the other hand, V-RF provides reliable connectivity even for larger distances. Such a heterogeneous

system has a great potential for increasing the quality-of-service (QoS) requirement of the vehicular communication system [6].

Moreover, the beyond fifth-generation (B5G) V2X communication networks require the support of massive connectivity and lower latency among vehicles and hence a new multiple access scheme needs to be adopted [7], [8]. The power-domain non-orthogonal multiple access (NOMA) [9] scheme has been extensively studied in recent years by allowing several users to access the same resource with distinctive power levels, thus increasing the spectral efficiency of the system. Additionally, it offers enlarged number of connectivity, lower access latency, and reduced resource collision. In comparison to orthogonal multiple access (OMA), NOMA achieves enhanced sum rates by utilizing successive interference cancellation (SIC) decoding at the receiver. The performance of optical power domain-NOMA (OPD-NOMA) in VLC based systems have recently attracted considerable research attention [10]–[17]. In order to improve quality-of-service (QoS) requirement, the cooperative techniques can be applied into NOMA networks. Cooperative technique is an effective solution to extend the coverage and overcome channel impairments such as fading, pathloss and shadowing. Depending on the cooperation types, there exists two main categories of cooperative NOMA (C-NOMA) techniques with user cooperation and dedicated relaying cooperation, respectively [18]. NOMA users collaborate as relays in the former, while in the latter category, dedicated relay nodes are distributed in the network. Several C-NOMA schemes have been discussed in the literature from various perspectives [18]–[20]. It is anticipated that the integration of cooperative techniques, NOMA, V-VLC, and V-RF systems can be exploited to improve the performance of V2X communication system with wider communication coverage, higher data rate, reduced transmission latency and increased spectral efficiency [21], [22].

1.1. Related Works

VLC is attractive because of its advantageous features such as large unlicensed bandwidth and high throughput with negligible interference from nearby users [23]–[25]. V-VLC is an outdoor application of VLC that complements the V-RF by employing the headlights and taillights of vehicles for communicating data between them [26]. Substantial research on V-VLC has been carried out using Lambertian path loss model which is built on the symmetrical radiation pattern of an LED source for indoor VLC scenarios [27]. A similar Lambertian model was used in [28] and [29] to study the VLC channel for vehicular communication. However, such a model was found to be inaccurate in low-beam and high-beam headlamps with asymmetrical distribution [30]–[34]. Abuella et al compared the Lambertian model with the simulated channel model in terms of received power as a function of distance [30]. It was shown that their simulated channel model is able to capture the reflections from the road, thus giving a reduced received power. In [31], three

different channel models are employed to analyse the asymmetrical distribution of the headlamps while considering the dynamic traffic conditions. The bit error rate (BER) performances of Lambertian, Gaussian and empirical path loss models were illustrated, revealing that the Lambertian model provides a lower BER as compared to the empirical model for the same SNR. In [32], the authors investigated the asymmetrical radiation pattern of the taillights from three different vehicles. They also compared the path loss for a proposed model with the existing Lambertian model. In [33], the authors investigated a realistic model for vehicular VLC communication by taking into account the low beam headlamp as the transmitter. It was observed that the inter-vehicular distance and the lateral distance between the transmitter and receiver plays a crucial role in the measurement of the channel model. Mehdi et al proposed a non-sequential ray tracing approach to study the asymmetrical radiation pattern of automotives for different weather conditions in [34]. The path loss curves are analysed for different aperture diameter in different weather conditions, and the results are then compared with the conventional Lambertian model.

Recently, researchers have been exploring the potential of a hybrid VLC-RF system in various applications [35]–[41]. For instance, in [35], the authors have explored the shortcomings that urban platooning faces due to the congestion in RF channel and investigated the use of VLC as an alternative. Zhang et al proposed a heterogeneous VLC/RF network by taking into the account the requirement of users and inter-cell interference limits for a small cell area [36]. In [37], the potential of employing energy efficient integrated VLC and RF system is discussed. In particular, the issue of power and bandwidth allocation to a heterogeneous VLC/RF based system is analyzed and further compared their results to only RF based systems. In [38], a message transmission system based on dual-hop VLC/ RF has been studied. Bao et al investigated an indoor VLC heterogeneous network system wherein VLC channel is integrated with RF channel for downlink and uplink communication [39]. Enhancement in capacity performance has been observed by comparing the VLC-HetNet results to that of RF. In [41], the coexistence of VLC and RF communication link for an indoor scenario has been investigated by utilizing performance metrics such as coverage probability and average rate for different network configurations.

Owing to spatial diversity gain, the packet reception probability of NOMA users can be significantly improved by combing copies from different paths [18]. In [42], a multiple antenna relaying network scenario is designed, where the receiving antennas at destinations employ maximal ratio combining (MRC). Further, the outage performance and ergodic sum rate of the users have been analysed to study the improvement in NOMA over OMA. In [43], the advantages of employing cooperative relay based PD-NOMA systems are analyzed. [44] investigated the concept of PD-NOMA for cellular future radio access and demonstrated that the downlink NOMA with SIC enhances the capacity and throughput of a cellular system. Furthermore, in [9],

	Our Paper	[58]-2022, [59]-2022	[17]-2021	[34]-2020	[60]-2019	[41]-2018
Hybrid RF-VLC based V2X	✓	✓				
Vehicle's headlights radiation pattern	✓			✓		
Cooperative-NOMA	✓				✓	
Maximal Ratio Combining (MRC)	✓				✓	
Stochastic Geometry Analysis	✓	✓	✓		✓	✓
Outage Probability	✓	✓	✓		✓	✓
Achievable Rate	✓		✓			✓

Table 1
Our novel contributions in contrast to the state-of-the-art.

the application of the NOMA scheme has been introduced into long-term evolution (LTE)-based V2X communication to improve the resource allocation schemes and to reduce latency. [45] investigated the performance analysis for a downlink NOMA network showing that NOMA has a better outage performance than OMA provided that the target rate and power allocation coefficient are wisely chosen. To expand the coverage of NOMA-based transmissions, one of the effective ways is to integrate the cooperative techniques into NOMA networks. In [19], the authors proposed a novel amplify-and-forward (AF)-based transmission protocol that involves both the user cooperation and the dedicated relay cooperation. [46] presented a comprehensive NOMA user relaying system, where near user close to base station can interplay between full duplex (FD) and half-duplex (HD) modes according to the channel conditions. Besides, Zhong *et.al* developed a full-duplex (FD) cooperative NOMA system with dual users, where a dedicated FD relays to support information transfer for users with weak channel conditions [47].

Stochastic geometry based approach, widely used for more than a decade, has been considered as an efficient mathematical tool to model and analyze the randomness of interference in V2X wireless communication [25], [48], [49]. To acknowledge the mathematical tractability and analytical modelling of vehicular ad hoc networks (VANETs), stochastic geometry has been employed in [50]. With the aid of stochastic geometry, the random positioning of interfering nodes are characterised by the Poisson point process [51]–[53]. In [54]–[57], the performance of NOMA enabled vehicular and UAV networks has been investigated using various analytical tools of stochastic geometry.

1.2. Motivation and Contributions

Against the aforementioned individual pros and cons of V-RF and V-VLC, this paper aims to exploit the complementary roles of these two technologies for enhanced V2X data exchanges at road intersection. Note that the existing V-RF solution advocates the use of message relaying at the center of intersection. However, with increase of vehicular density, V-RF tends to suffer from larger communication latency and reduced packet delivery rates due to channel congestion. In this paper, we propose to use NOMA enabled hybrid V-VLC/V-RF communication systems to address this problem. In particular, the main motivation is to mitigate the effects of shadowing caused by blockages[1] such as building and other obstructions at road intersection. Moreover, such a scheme can also facilitate more reliable communication in the case of non-line-of-sight (NLoS) transmission. Our novel contributions against previously published works are shown in Table I. More specifically, the main contributions of this research paper are summarized as follows:

1. We explore a cooperative NOMA enabled hybrid V-VLC/V-RF solution for improving safety message dissemination and enabling massive connectivity among vehicles particularly at road intersection scenario. The superiority of the proposed V2X solution is validated by comparing it with conventional V-RF communication system.

2. We develop tractable analytical expression for such NOMA enabled hybrid vehicular communication system in terms of outage probability and average achievable rate using various analytical tools of stochastic geometry. The proposed analysis is then extended to generic NOMA scheme with K destination vehicles, where $K > 2$.

3. We also examine the impact of vehicles headlights radiation pattern viz. Lambertian and empirical path

---

[1]Empirical measurements showed that due to such blockages, the strength of received V2V signal drops rapidly over distance away from the intersection [61]. As a consequence, vehicles located in perpendicular streets may not be able to communicate well with each other, resulting in a significant decrease in V2V communication performance.
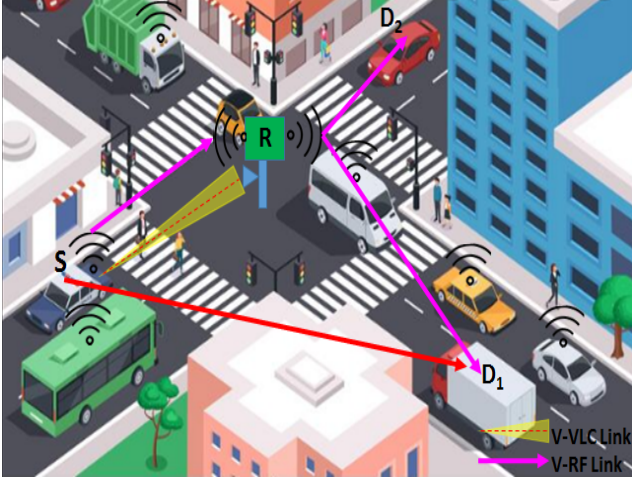
Figure 1: Real life application scenario: At road intersection, vehicles in blocked LOS (dashed red line) can communicate via C-NOMA supported hybrid V-VLC/V-RF systems. The SR link can either be V-VLC (red color line) or V-RF (solid magenta line) link, while $RD_{1,2}$ link is a V-RF link.
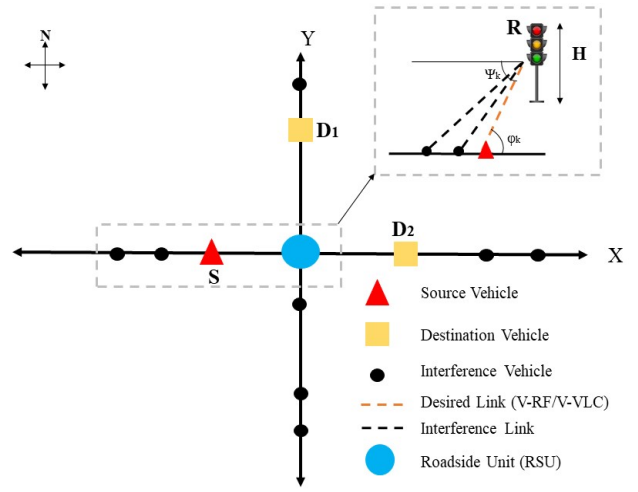

Figure 2: Abstraction model of the considered scenario. The source vehicle is marked with red triangle, destination vehicles are marked with yellow squares, and interfering vehicles with black circles. The desired link is represented by red dotted line and the interference link is represented by black dotted line. H denotes the height of the traffic light.

loss model on statistical characterization of the proposed hybrid solution. Moreover, we compare the performance of NOMA with conventional OMA scheme and show that NOMA leads to improved performance for the proposed system.

1.3. Paper Organization

The structure of the paper is organized as follows. In Section II, we describe the network scenario and state the assumptions used for our analysis. A detailed analytical framework to characterize the hybrid based V-VLC/V-RF system in terms of outage probability and average achievable rate are discussed in section III. In section IV, the results and the related discussions are analyzed. Finally, the concluding remarks and the future work is provided in Section V.

Notation: $|| \cdot ||$ denotes euclidean norm, $\mathbb{P}[\cdot]$ denotes probability of an event, $\mathbb{E}_Y[\cdot]$ is the expectation of its argument over random variable (RV) Y. $\mathbb{R}^1$ denote one dimensional space. $\mathcal{F}_X(\cdot)$ and ξ_c denote cumulative distribution function and complementary error function respectively. $\varphi \sim$ 1D-HPPP denotes one-dimensional homogeneous Poisson point process.

2. System Model and Assumptions

2.1. Network Scenario

A typical road intersection scenario involving cooperative NOMA transmission between a source vehicle, S and two destination vehicles, D_1 and D_2 with the help of a relay node, R has been shown in Fig. 1. The proposed analysis can been extended to generalized form for K destination vehicles where $K > 2$. The relay node is assumed to be kept at the road intersection, where the two perpendicular roads, horizontal road X and vertical road Y, cross each other. We assume the communication from a single source vehicle to

multiple destination vehicles applying decode and forward (DF) strategy via relay node [62]. For sake of analysis, we consider a realistic scenario, where all the destination vehicles do not require the same amount of data rate, that is, D_1 can be a vehicle which needs to be served immediately with a lower data rate whereas D_2 has a lower priority with a higher data rate[2]. As per insights shared in [67], we also consider that vehicles can control the transmit power of optical signals. Half duplex transmission is employed where the transmission occurs in two phases. In the first phase, reception occurs where R, D_1 and D_2 receives the message from S ($S \rightarrow R$, $S \rightarrow D_1$, $S \rightarrow D_2$) and in the second phase, the message received at R is broadcasted to the destination vehicles D_1 and D_2 ($R \rightarrow D_1$, $R \rightarrow D_2$). Each of these phases lasts one time slot and the message received at D_1 and D_2 in the two phases are decoded after MRC. Fig. 2 provides an abstract model of the proposed network scenario.

A hybrid VLC-RF based V2X scenario is considered, where SR link can be either VLC link or an RF link, while SD and RD are RF links as shown in Fig.3. A hybrid transmission without MRC implies that the communication takes place between $S \rightarrow R$ and $R \rightarrow D$, whereas the hybrid transmission with MRC implies that the communication occurs between $S \rightarrow R$, $R \rightarrow D$ and $S \rightarrow D$. During $S \rightarrow R$ transmission, only one of the links is operational at a given time instant based on QoS requirement. For instance, when SIR of V-VLC link is above a threshold value, the system keeps on operating with V-VLC link. However, as distance of the source vehicle S from R becomes large, the quality of V-VLC link degrades, as a consequence V-RF link is then

---

[2]Unlike [20], [63], we consider a more realistic assumption that the destination vehicular nodes are prioritize according to their quality of service (QoS) requirements as reported in [64]–[66].
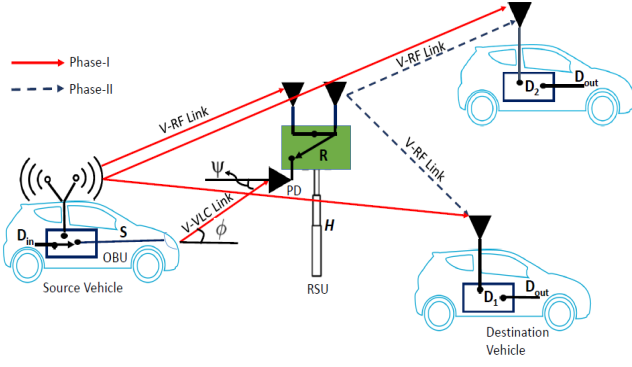
Figure 3: Illustration of cooperative NOMA aided hybrid VLC-RF based V2X with relaying.

activated. The SR link goes to outage only when both V-VLC and V-RF link falls in outage [59].

The triplet set $\{S, R, D\}$ are subject to interference that are originated from vehicles on roads. The set of interfering vehicles can be denoted by φ_X and φ_Y on X and Y road respectively. These are distributed according to 1D-HPPP, expressed as, $\varphi_X \sim$ 1D-HPPP (λ_X, x) and $\varphi_Y \sim$ 1D-HPPP(λ_Y, y), where x and λ_X and y and λ_Y are the position of interfering vehicles and their intensity on the X and Y road respectively. We assume that the vehicular nodes employ slotted Aloha protocol with parameter ρ, where each node can access the medium with an access probability ρ.

2.2. Channel Model for V-VLC and V-RF

We assume V-VLC system consists of a transmitting LED headlamp and a PD receiver placed at the back end of the vehicle. The channel impulse response which have been used in outdoor environment for a Lambertian source is given as [17],

$$h_k = \frac{(\xi + 1)A}{2\pi D_k^2} \cos^\xi(\phi_k) \cos(\psi_k) T_s(\psi_k) g(\psi_k), \quad (1)$$

where ξ represents the Lambertian order expressed as, $\xi = -\frac{\ln(2)}{\ln(\cos\phi_{\frac{1}{2}})}$, $\phi_{\frac{1}{2}}$, A, ϕ_k, ψ_k, $T_s(\psi_k)$, and D_k denote the LED half beam angle, area of the PD, angle of arrival, angle of irradiance, the gain of the optical filter at the receiver and euclidean distance between the kth vehicle and the intersection respectively. The gain of optical concentrator at the receiver, $g(\psi_k)$ is expressed as,

$$g(\psi_k) = \begin{cases} \frac{n^2}{\sin^2 \psi_F}; & \text{if } 0 \leq \phi_k \leq \psi_F, \\ 0; & \text{if } \phi_k > \psi_F, \end{cases} \quad (2)$$

where n denotes the refractive index of the optical concentrator and ψ_F is field of view (FOV).

In this study, we consider Empirical modelling based realistic asymmetrical angular distribution of the radiation intensity pattern of light source. Assuming no attenuation loss, the channel DC gain for V-VLC system can be given as

[34],

$$H(0) = \left(\frac{D_R \cos(\psi_i)^{\frac{1}{\varepsilon}}}{\zeta L_i} \right)^2 \quad (3)$$

where D_R and ψ denote the aperture diameter and angle of irradiance. Here, $\cos \psi_i = \frac{d_i}{\sqrt{d_i^2 + H^2}}$ and d_i is the distance between i^{th} transmitter and the intersection. The two correction coefficients (ε and ζ) take into account the asymmetrical pattern of the headlamp and weather conditions [34]. $L_i = \sqrt{d_i^2 + H^2}$ which is expressed as the propagation distance between the ith transmitter to the relay.

For V-RF communication, the fading coefficient for the links source-to-relay, source-to-destination and relay-to-destination denoted by, h_{SR}, h_{SD} and h_{RD} respectively are modeled as $\sim \mathcal{N}(0, 1)$. Given a RF link, the power fading coefficient ($|h_{SR}|^2, |h_{SD}|^2, |h_{RD}|^2$) is an exponential random variable with unit mean. Further, we consider a path loss model l_{pq} between the nodes p and q. For direct LOS between p and q, $l_{pq} = \|p - q\|_2^{-\alpha}$ where $\|p - q\|$ is the euclidean distance between node p and q, where $\|.\|_2$ is l_2 norm, and α is the path loss exponent. For non-line-of-sight propagation (NLOS), Manhattan model is used where $l_{xy} = \|p - q\|_1^{-\alpha}$ where $\|.\|_1$ is l_1 norm[68]. For our case, the distance of vehicles from relay node is represented as, $(\sqrt{H^2 + d^2})^{-\alpha}$, where d is the distance of the vehicle from the intersection point and H is the height of relay.

The signal transmitted by source S, denoted by X_S, is a combination of the data intended to vehicular nodes D_1 and D_2,

$$X_S = \sqrt{a_1} X_{D_1} + \sqrt{a_2} X_{D_2}, \quad (4)$$

where a_1 and a_2 are the power allocation coefficient to vehicular nodes D_1 and D_2 such that $a_1 + a_2 = 1$. Here X_{D_1} and X_{D_2} are the signals intended to the destination nodes D_1 and D_2.

For V-VLC system, the received optical signal at R due to VLC link, denoted as Y_R^{VLC}, can be given as,

$$Y_R^{VLC} = \mathcal{R} h X_S + \sqrt{I_{VLC}}, \quad (5)$$

where $\mathcal{R}$ denotes the responsivity of PD, and I_{VLC} is the combined interference experienced at the relay node R from vehicles in adjacent lanes. It can be given as,

$$I_{VLC} = \sum_{r_i \in \varphi} z \frac{P_{VLC} r_i^{\frac{4}{\varepsilon}}}{(H^2 + r_i^2)^{\frac{2\varepsilon + 2}{\varepsilon}}}, \quad (6)$$

where $z = \mathcal{R}^2 \left(\frac{D_R}{\zeta} \right)^4$, r_i is the distance of interfering vehicles from intersection and P_{VLC} denotes the transmission power for VLC.

For V-RF link, the signal received at relay node R during $S \rightarrow R$ transmission, denoted as Y_R^{RF}, can be expressed as,

$$Y_R^{RF} = h_{SR}\sqrt{l_{SR}}X_S + \sum_{x\in\varphi_{X_R}} h_{Rx}\sqrt{l_{Rx}}X_x$$
$$+ \sum_{y\in\varphi_{Y_R}} h_{Ry}\sqrt{l_{Ry}}X_y, \quad (7)$$

where X_x and X_y represent the message transmitted by the interfering nodes x and y respectively and l_{Rx} and l_{Ry} denote the path loss model between vehicular node R and interfering node x or y. The signal received at the vehicular node D_i during $S \to D_i$ transmission, denoted as Y_{D_i}, can be given as,

$$Y_{D_i} = h_{SD_i}\sqrt{l_{SD_i}}X_S + \sum_{x\in\varphi_{X_{D_i}}} h_{D_i x}\sqrt{l_{D_i x}}X_x$$
$$+ \sum_{y\in\varphi_{Y_{D_i}}} h_{D_i y}\sqrt{l_{D_i y}}X_y, \quad (8)$$

where $l_{D_i x}$ denotes the path loss model between vehicular node D_i and interfering node x. The signal received at vehicular node D_i during $R \to D_i$ transmission, denoted as Y_{RD_i}, can be represented as,

$$Y_{RD_i} = h_{RD_i}\sqrt{l_{RD_i}}X_R + \sum_{x\in\varphi_{X_{D_i}}} h_{D_i x}\sqrt{l_{D_i x}}X_x$$
$$+ \sum_{y\in\varphi_{Y_{D_i}}} h_{D_i y}\sqrt{l_{D_i y}}X_y. \quad (9)$$

3. PERFORMANCE ANALYSIS

In the following, we evaluate the performance of the system model using outage probability and average achievable rate as the performance metrics.

3.1. Outage Probability for V-VLC

An outage is said to occur when the instantaneous SINR drops below a certain threshold value. For an interference limited scenario, we first evaluate the SIR at each of the receiving nodes, and then define outage probability associated with them. The vehicular node D_1 is assumed to receive information with higher power than node D_2, therefore it will decode first according to SIC decoding and interference would be due to D_2. The SIR at R due to VLC link, denoted as $\gamma_{SR_1}^{VLC}$, can be expressed as,

$$\gamma_{SR_1}^{VLC} = \frac{za_1 P_{VLC}d_0^{\frac{4}{\varepsilon}}(H^2 + d_0^2)^{-(\frac{2\varepsilon+2}{\varepsilon})}}{za_2 P_{VLC}d_0^{\frac{4}{\varepsilon}}(H^2 + d_0^2)^{-(\frac{2\varepsilon+2}{\varepsilon})} + I_{VLC}}, \quad (10)$$

where d_0 is the distance between source node S and relay node R.

The relay R will first retrieve the information from D_1

vehicle, denoted as $\gamma_{SR_{2-1}}^{VLC}$, is expressed as[3],

$$\gamma_{SR_{2-1}}^{VLC} = \frac{za_1 P_{VLC}d_0^{\frac{4}{\varepsilon}}(H^2 + d_0^2)^{-(\frac{2\varepsilon+2}{\varepsilon})}}{za_2 P_{VLC}d_0^{\frac{4}{\varepsilon}}(H^2 + d_0^2)^{-(\frac{2\varepsilon+2}{\varepsilon})} + I_{VLC}}. \quad (11)$$

The SIR at relay node to decode the data associated with vehicular node D_2, denoted as $\gamma_{SR_2}^{VLC}$, is represented as,

$$\gamma_{SR_2}^{VLC} = \frac{za_2 P_{VLC}d_0^{\frac{4}{\varepsilon}}(H^2 + d_0^2)^{-(\frac{2\varepsilon+2}{\varepsilon})}}{I_{VLC}}. \quad (12)$$

Let us denote the outage event associated with vehicular node D_1 at R as $O_{SR_1}^{VLC}$. The outage event at R when vehicular node D_2 is unable to retrieve the data associated with D_1 is denoted as $O_{SR_{2-1}}^{VLC}$. The outage at R when D_2 node is unable to retrieve its own data is denoted by $O_{SR_2}^{VLC}$. These outage events can be expressed as,

$$O_{SR_1}^{VLC} = \{\gamma_{SR_1}^{VLC} < \theta_1\},$$
$$O_{SR_{2-1}}^{VLC} = \{\gamma_{SR_{2-1}}^{VLC} < \theta_1\}, \quad (13)$$
$$O_{SR_2}^{VLC} = \{\gamma_{SR_2}^{VLC} < \theta_2\},$$

where $\theta_1 = \frac{2\pi}{e}(2^{C_1} - 1)$ and $\theta_2 = \frac{2\pi}{e}(2^{C_2} - 1)$ and C_1 and C_2 are the target data rates of vehicular nodes D_1 and D_2 respectively.

We now calculate the outage probability associated with the relay node R by using the moment generating functional (MGF) approach. The outage probability at R due to vehicular node D_1, denoted as $P_{O_{R_1}}^{VLC}$, can be calculated by using [58, Eq. (19)],

$$P_{O_{R_1}}^{VLC} \approx 1 - \frac{2^{-F}\exp\left(\frac{E}{2}\right)}{\theta_1^{-1}} \sum_{f=0}^{F} \binom{F}{f} \sum_{g=0}^{G+f} \frac{(-1)^g}{H_g} Re\left(\frac{\mathcal{L}_Z(s)}{s}\right). \quad (14)$$

In (14), $\mathcal{L}_Z(s)$ denotes Laplace transform of the probability distribution of a random variable, Z which can be expressed as [17, Eq. 23],

$$\mathcal{L}_Z(s) =$$

$$\mathbb{E}_I\left\{\exp\left(-\frac{sI_{VLC}}{z(a_1 - \theta_1 a_2)P_{VLC}d_0^{\frac{4}{\varepsilon}}(H^2 + d_0^2)^{-(\frac{2\varepsilon+2}{\varepsilon})}}\right)\right\}$$

$$= \mathbb{E}_r\left\{\prod_{i=1}^{N}\exp\left(-\frac{s}{z(a_1 - \theta_1 a_2)d_0^{\frac{4}{\varepsilon}}(H^2 + d_0^2)^{-(\frac{2\varepsilon+2}{\varepsilon})}}\right.\right.$$

---

[3]Perfect SIC has been considered which implies that there is no fraction of power left after SIC decoding process [60].

$$\times \frac{zr_i^{\frac{4}{\varepsilon}}}{(H^2 + r_i^2)^{\frac{2\varepsilon+2}{\varepsilon}}}\Bigg)\Bigg)\Bigg\}.$$

(15)

The expectation in (15) can be solved using probability generating functional laplace (PGFL) defined for a homogeneous Poisson point process [69].

$$\mathbb{E}_r\Bigg\{\prod_{i=1}^{N}\exp\Bigg(-\frac{s}{z(a_1 - \theta_1 a_2)d_0^{\frac{4}{\varepsilon}}(H^2 + d_0^2)^{-(\frac{2\varepsilon+2}{\varepsilon})}}$$

$$\times \frac{zr_i^{\frac{4}{\varepsilon}}}{(H^2 + r_i^2)^{\frac{2\varepsilon+2}{\varepsilon}}}\Bigg)\Bigg\}$$

$$= \exp\Bigg[-\rho\lambda_D\int_{d_0}^{\infty}\Bigg(1 - \exp\Bigg(-\frac{s}{z(a_1 - \theta_1 a_2)}$$

$$\times\frac{zr^{\frac{4}{\varepsilon}}}{d_0^{\frac{4}{\varepsilon}}(H^2 + d_0^2)^{-(\frac{2\varepsilon+2}{\varepsilon})}(H^2 + r^2)^{\frac{2\varepsilon+2}{\varepsilon}}}\Bigg)\Bigg)dr\Bigg], \quad (16)$$

where λ_D denotes the intensity of the interfering vehicles located on the roads. Eq.(16) can be solved using numerical methods that can be implemented using MATLAB. The outage probability at R associated with vehicular node D_2 can be calculated by using [17, Eq.(27)],

$$P_{O_{R_2}}^{VLC} =$$

$$= 1 - \mathbb{P}\Bigg(\frac{I_{VLC}}{zP_{VLC}d_0^{\frac{4}{\varepsilon}}(H^2 + d_0^2)^{-(\frac{2\varepsilon+2}{\varepsilon})}} < \min(B_1, B_2)\Bigg),$$

(17)

where $B_1 = \frac{(a_1 - \theta_1 a_2)}{\theta_1}$ and $B_2 = \frac{a_2}{\theta_2}$.

Now, we extend the NOMA results to K vehicular nodes. The SIR at relay R associated with D_i to decode D_w due to the VLC link can be expressed as,

$$\gamma_{SR_i}^{VLC} = \frac{za_i P_{VLC}d_0^{\frac{4}{\varepsilon}}(H^2 + d_0^2)^{-(\frac{2\varepsilon+2}{\varepsilon})}}{zP_{VLC}d_0^{\frac{4}{\varepsilon}}(H^2 + d_0^2)^{-(\frac{2\varepsilon+2}{\varepsilon})}\Bigg[\sum_{u=w+1}^{K}a_u\Bigg] + I_{VLC}},$$

(18)

here, when $u > K$, then $\sum_{u=w+1}^{K}a_u = 0$. Then, the outage probability at node R_i is expressed as [17],

$$P_{O_{R_i}}^{VLC} =$$

$$\begin{cases} 1 - \mathbb{P}\Bigg(\dfrac{I_{VLC}}{zP_{VLC}d_0^{\frac{4}{\varepsilon}}(H^2+d_0^2)^{-(\frac{2\varepsilon+2}{\varepsilon})}} < B_{(i)_{\min}}\Bigg); & \text{else,} \\[4ex] 1; & \bigcup\limits_{w=1}^{K}\dfrac{a_w}{\sum\limits_{u=w+1}^{K}a_u} < \theta_w, \end{cases}$$

(19)

where $B_{(i)_{\min}}$ is given by (20).

3.2. Outage Probability for V-RF

We define the SIR at R due to D_1 as $\gamma_{SR_1}^{RF}$, expressed as,

$$\gamma_{SR_1}^{RF} = \frac{P_{RF}|h_{SR}|^2 l_{SR}a_1}{P_{RF}|h_{SR}|^2 l_{SR}a_2 + I_{X_R} + I_{Y_R}}, \quad (21)$$

where P_{RF} is the RF transmission power and I_{X_M} and I_{Y_M} denote the combined interference from perpendicular roads X and Y at M respectively. Here M signifies the receiving nodes, $M \in \{R, D_1, D_2\}$. I_{X_M} and I_{Y_M} can be expressed as,

$$I_{X_M} = \sum_{x\in\varphi_{X_M}} P_{RF}|h_{M_x}|^2 l_{M_x},$$

$$I_{Y_M} = \sum_{y\in\varphi_{Y_M}} P_{RF}|h_{M_y}|^2 l_{M_y}. \quad (22)$$

The SIR at relay node R to first retrieve the information from D_1, denoted as $\gamma_{SR_{2-1}}^{RF}$, can be expressed as,

$$\gamma_{SR_{2-1}}^{RF} = \frac{P_{RF}|h_{SR}|^2 l_{SR}a_1}{P_{RF}|h_{SR}|^2 l_{SR}a_2 + I_{X_R} + I_{Y_R}}. \quad (23)$$

The SIR at node R associated with D_2 to retrieve its own data, denoted as $\gamma_{SR_2}^{RF}$, can be represented as,

$$\gamma_{SR_2}^{RF} = \frac{P_{RF}|h_{SR}|^2 l_{SR}a_2}{I_{X_R} + I_{Y_R}}. \quad (24)$$

Let us denote the outage event at R associated with vehicular node D_1 as $O_{SR_1}^{RF}$. Let $O_{SR_{2-1}}^{RF}$ be the outage event at R when vehicular node D_2 cannot retrieve the message associated with D_1. The outage at R when D_2 vehicle is unable to decode its own data is denoted by $O_{SR_2}^{RF}$. These outage events can be expressed as,

$$\begin{aligned} O_{SR_1}^{RF} &= \{\gamma_{SR_1}^{RF} < \beta_1\}, \\ O_{SR_{2-1}}^{RF} &= \{\gamma_{SR_{2-1}}^{RF} < \beta_1\}, \\ O_{SR_2}^{RF} &= \{\gamma_{SR_2}^{RF} < \beta_2\}, \end{aligned} \quad (25)$$

where $\beta_1 = 2^{2C_1} - 1$ and $\beta_2 = 2^{2C_2} - 1$.

Having analysed these expressions, we now calculate the outage probability at relay node R associated with vehicular

$$B_{(i)_{\min}} =$$

$$\min\left(\frac{a_{i-(K-1)} - \theta_{i-(K-1)}\left[\sum_{u=i-(K-1)+1}^{K} a_u\right]}{\theta_{i-(K-1)}}, \frac{a_{i-(K-2)} - \theta_{i-(K-2)}\left[\sum_{u=i-(K-2)+1}^{K} a_u\right]}{\theta_{i-(K-2)}}, ..., \frac{a_{i-(K-L)} - \theta_{i-(K-L)}\left[\sum_{u=i-(K-L)+1}^{K} a_u\right]}{\theta_{i-(K-L)}}\right), \quad (20)$$

where $L \in (1, 2, ..., K)$ and we set the condition that $L > K - 1$.

---

nodes D_1 and D_2. The outage probability at R associated with D_1 node, denoted as $P_{O_{R_1}}^{RF}$, can be represented as [70],

$$P_{O_{R_1}}^{RF} = \mathbb{P}(\gamma_{SR_1}^{RF} < \beta_1)$$

$$= 1 - \mathcal{L}_{I_{X_R}}\left(\frac{A_1}{P_{RF}l_{SR}}\right)\mathcal{L}_{I_{Y_R}}\left(\frac{A_1}{P_{RF}l_{SR}}\right), \quad (26)$$

where $A_1 = \frac{\beta_1}{a_1 - \beta_1 a_2}$ and $\mathcal{L}_{I_{X_R}}$ and $\mathcal{L}_{I_{Y_R}}$ denotes the Laplace transforms of the interfering vehicles at relay node R from road X and Y whose expressions can be calculated by using [58, Eq. (33)] as,

$$\mathcal{L}_{I_{X_R}}(s) = \exp\left(\frac{-\rho\lambda_X\pi s P_{RF}}{\sqrt{H^2 + sP_{RF}}}\right),$$

$$\mathcal{L}_{I_{Y_R}}(s) = \exp\left(\frac{-\rho\lambda_Y\pi s P_{RF}}{\sqrt{H^2 + sP_{RF}}}\right). \quad (27)$$

Eq. (26) can be expressed in simplified form as,

$$P_{O_{R_1}}^{RF} = \begin{cases} 1 - \mathcal{G}_R\left(\frac{A_1}{P_{RF}l_{SR}}\right); & \text{otherwise,} \\ 1; & \beta_1 \geq \frac{a_1}{a_2}, \end{cases} \quad (28)$$

where $\mathcal{G}_M(\frac{C}{D}) = \mathcal{L}_{I_{X_M}}\left(\frac{C}{D}\right)\mathcal{L}_{I_{Y_M}}\left(\frac{C}{D}\right)$.
Similarly, the outage probability at R associated with vehicular node D_2, denoted as $P_{O_{R_2}}^{RF}$, can be represented as,

$$P_{O_{R_2}}^{RF} = \begin{cases} 1 - \mathcal{G}_R\left(\frac{A_{\max}}{P_{RF}l_{SR}}\right); & \text{otherwise,} \\ 1; & \beta_2 \geq \frac{a_1}{a_2}, \end{cases} \quad (29)$$

where $A_2 = \frac{\beta_2}{a_2}$ and $A_{\max} = \max(A_1, A_2)$.
Assuming that V-VLC and V-RF links to be independent, the overall outage performance at relay node R associated with vehicular nodes D_1 and D_2, denoted as $P_{O_{R_i}}$ where i $\in$ {1,2}, can be expressed as,

$$P_{O_{R_i}} = P_{O_{R_i}}^{RF} \times P_{O_{R_i}}^{VLC}. \quad (30)$$

The SIR at destination node D_1 to retrieve its own data when transmission occurs from $R \rightarrow D_1$ is expressed as,

$$\gamma_{RD_1} = \frac{P_{RF}|h_{RD_1}|^2 l_{RD_1} a_1}{P_{RF}|h_{RD_1}|^2 l_{RD_1} a_2 + I_{X_{D_1}} + I_{Y_{D_1}}}. \quad (31)$$

Now, as D_2 comes second in decoding order, it first retrieves the data associated with D_1 vehicle. The SIR, denoted as $\gamma_{RD_{2-1}}$, can be expressed as,

$$\gamma_{RD_{2-1}} = \frac{P_{RF}|h_{RD_2}|^2 l_{RD_2} a_1}{P_{RF}|h_{RD_2}|^2 l_{RD_2} a_2 + I_{X_{D_2}} + I_{Y_{D_2}}}. \quad (32)$$

The SIR at node D_2 to retrieve its own data can be represented as,

$$\gamma_{RD_2} = \frac{P_{RF}|h_{RD_2}|^2 l_{RD_2} a_2}{I_{X_{D_2}} + I_{Y_{D_2}}}. \quad (33)$$

Let O_{RD_1} be the outage event associated with D_1. The outage event when D_2 node is unable to retrieve the data associated with vehicular node D_1, denoted as $O_{RD_{2-1}}$. The outage when destination node D_2 is unable to decode its own data is denoted by O_{RD_2}. These outage events can be represented as,

$$\begin{aligned} O_{RD_1} &= \{\gamma_{RD_1} < \beta_1\}, \\ O_{RD_{2-1}} &= \{\gamma_{RD_{2-1}} < \beta_1\}, \\ O_{RD_2} &= \{\gamma_{RD_2} < \beta_2\}. \end{aligned} \quad (34)$$

The outage probability associated with vehicular node D_1, denoted as $P_{O_{RD_1}}$, can be expressed as [70],

$$P_{O_{RD_1}} = \mathbb{P}(\gamma_{RD_1} < \beta_1)$$

$$= 1 - \mathcal{L}_{I_{X_{D_1}}}\left(\frac{A_1}{P_{RF}l_{RD_1}}\right)\mathcal{L}_{I_{Y_{D_1}}}\left(\frac{A_1}{P_{RF}l_{RD_1}}\right), \quad (35)$$

where $\mathcal{L}_{I_{X_M}}$ and $\mathcal{L}_{I_{Y_M}}$ denotes the Laplace transforms of the interfering vehicles at destination nodes, D_1 and D_2, from road X and Y whose expressions are governed by [60, Eq.(21), Eq.(22)].
Similarly, the outage probability associated with vehicular node D_2, denoted as $P_{O_{RD_2}}$, can be expressed as,

$$P_{O_{RD_2}} = 1 - \mathbb{P}(\gamma_{RD_{2-1}} < \beta_1) \times \mathbb{P}(\gamma_{RD_2} < \beta_2)$$

$$= 1 - \mathcal{L}_{I_{X_{D_2}}}\left(\frac{A_{\max}}{P_{RF}l_{RD_2}}\right)\mathcal{L}_{I_{Y_{D_2}}}\left(\frac{A_{\max}}{P_{RF}l_{RD_2}}\right), \quad (36)$$

The overall outage probability associated with nodes D_1

and D_2 for a hybrid transmission without MRC, denoted as P_{Outage,D_i} where $i \in \{1,2\}$, can be expressed as,

$$P_{Outage,D_i} = 1 - (1 - P_{O_{R_i}}) \times (1 - P_{O_{RD_i}}).$$ (37)

During the second phase, after applying MRC at destination node D_1, the SIR associated with D_1 can be expressed as,

$$\gamma_{D_1} = \frac{P_{RF}(|h_{SD_1}|^2 l_{SD_1} + |h_{RD_1}|^2 l_{RD_1})a_1}{P_{RF}(|h_{SD_1}|^2 l_{SD_1} + |h_{RD_1}|^2 l_{RD_1})a_2 + I_{X_{D_1}} + I_{Y_{D_1}}}.$$ (38)

Similarly, in the second phase, after applying MRC, D_2 first retrieves the message associated with D_1 vehicle. Hence, the SIR at node D_2 to interpret D_1 can be represented as,

$$\gamma_{D_{2-1}} = \frac{P_{RF}(|h_{SD_2}|^2 l_{SD_2} + |h_{RD_2}|^2 l_{RD_2})a_1}{P_{RF}(|h_{SD_2}|^2 l_{SD_2} + |h_{RD_2}|^2 l_{RD_2})a_2 + I_{X_{D_2}} + I_{Y_{D_2}}}.$$ (39)

Now, the SIR at node D_2 to retrieve its own data after MRC reception, can be expressed as,

$$\gamma_{D_2} = \frac{P_{RF}(|h_{SD_2}|^2 l_{SD_2} + |h_{RD_2}|^2 l_{RD_2})a_2}{I_{X_{D_2}} + I_{Y_{D_2}}}.$$ (40)

We assume O_{D_1} is the outage event associated with D_1. The outage event when D_2 is unable to retrieve the message associated with D_1, denoted as $O_{D_{2-1}}$. The outage when D_2 is unable to retrieve its own message is denoted by $O_{D_{2-2}}$. These outage events can be given as,

$$O_{D_1} = \{\gamma_{D_1} < \beta_1\},$$
$$O_{D_{2-1}} = \{\gamma_{D_{2-1}} < \beta_1\},$$ (41)
$$O_{D_2} = \{\gamma_{D_2} < \beta_2\}.$$

We now calculate the outage probability related to vehicular nodes D_1 and D_2. The outage probability associated with D_1 destination node, denoted by $P_{O_{D_1}}$, can be represented as [60],

$$P_{O_{D_1}} = \mathbb{P}(\gamma_{D_1} < \beta_1)$$

$$= 1 - \left\{ \frac{l_{RD_1} \mathcal{G}_{D_1}\left(\frac{A_1}{P_{RF} l_{RD_1}}\right) - l_{SD_1} \mathcal{G}_{D_1}\left(\frac{A_1}{P_{RF} l_{SD_1}}\right)}{l_{RD_1} - l_{SD_1}} \right\}.$$ (42)

The outage probability associated with D_2 destination node, denoted by $P_{O_{D_2}}$, can be expressed as,

$$P_{O_{D_2}} = 1 - \mathbb{P}(\gamma_{D_{2-1}} < \beta_1) \times \mathbb{P}(\gamma_{D_2} < \beta_2)$$

$$= 1 - \left\{ \frac{l_{RD_2} \mathcal{G}_{D_2}\left(\frac{A_{max}}{P_{RF} l_{RD_2}}\right) - l_{SD_2} \mathcal{G}_{D_2}\left(\frac{A_{max}}{P_{RF} l_{SD_2}}\right)}{l_{RD_2} - l_{SD_2}} \right\}.$$ (43)

The overall outage probability associated with vehicular nodes D_1 and D_2 after applying MRC, denoted as P_{Outage,D_i}^{MRC} where $i \in \{1,2\}$, can be expressed as,

$$P_{Outage,D_i}^{MRC} = 1 - (1 - P_{O_{R_i}}) \times (1 - P_{O_{D_i}}).$$ (44)

Now, we extend the NOMA results to K vehicular nodes. The SIR at relay R associated with D_i to decode the message related to D_w can be represented as,

$$\gamma_{SR_{i \to w}}^{RF} = \frac{P_{RF}|h_{SR}|^2 l_{SR} a_i}{P_{RF}|h_{SR}|^2 l_{SR}\left[\sum\limits_{u=w+1}^{K} a_u\right] + I_{X_R} + I_{Y_R}}.$$ (45)

The outage probability related to R due to RF link can be expressed as [17],

$$P_{O_{R_i}}^{RF} = \begin{cases} 1 - \mathcal{G}_R\left(\frac{A_{(i)max}}{P_{RF} l_{SR}}\right); & \text{otherwise,} \\ 1; & \bigcup\limits_{w=1}^{K} \frac{a_w}{\sum\limits_{u=w+1}^{K} a_u} < \beta_w, \end{cases}$$ (46)

where $A_{(i)max}$ is given by (47).

The expression for SIR at destination node D_i to decode D_w data during $R \to D_i$ transmission, denoted as $\gamma_{RD_{i \to w}}$, can be given as,

$$\gamma_{RD_{i \to w}} = \frac{P_{RF}|h_{RD_i}|^2 l_{RD_i} a_i}{P_{RF}|h_{RD_i}|^2 l_{RD_i}\left[\sum\limits_{u=w+1}^{K} a_u\right] + I_{X_{D_i}} + I_{Y_{D_i}}}.$$ (48)

The outage probability related to vehicular node D_i, denoted as $P_{O_{RD_i}}$, can be represented as,

$$P_{O_{RD_i}} = \begin{cases} 1 - \mathcal{G}_{D_i}\left(\frac{A_{(i)max}}{P_{RF} l_{RD_i}}\right); & \text{otherwise,} \\ 1; & \bigcup\limits_{w=1}^{K} \frac{a_w}{\sum\limits_{u=w+1}^{K} a_u} < \beta_w. \end{cases}$$ (49)

During the second phase, after applying MRC, the SIR related to node D_i to retrieve message associated with node D_w, denoted as $\gamma_{D_{i \to w}}$, can be expressed as,

$$\gamma_{D_{i \to w}} =$$

$$\frac{P_{RF}(|h_{SD_i}|^2 l_{SD_i} + |h_{RD_i}|^2 l_{RD_i})a_i}{P_{RF}(|h_{SD_i}|^2 l_{SD_i} + |h_{RD_i}|^2 l_{RD_i})\left[\sum\limits_{u=w+1}^{K} a_u\right] + I_{X_{D_i}} + I_{Y_{D_i}}}.$$ (50)

The outage probability related to vehicular node D_i can be expressed as [60],

$$P_{O_{D_i}} = 1 - \left\{ \frac{l_{RD_i} \mathcal{G}_{D_i}\left(\frac{A_{(i)max}}{P_{RF} l_{RD_i}}\right) - l_{SD_i} \mathcal{G}_{D_i}\left(\frac{A_{(i)max}}{P_{RF} l_{SD_i}}\right)}{l_{RD_i} - l_{SD_i}} \right\}.$$ (51)

$$A_{(i)_{max}} =$$

$$\max\left(\frac{\beta_{i-(K-1)}}{a_{i-(K-1)} - \beta_{i-(K-1)}\left[\sum_{u=i-(K-1)+1}^{K} a_u\right]}, \frac{\beta_{i-(K-2)}}{a_{i-(K-2)} - \beta_{i-(K-2)}\left[\sum_{u=i-(K-2)+1}^{K} a_u\right]}, ..., \frac{\beta_{i-(K-L)}}{a_{i-(K-L)} - \beta_{i-(K-L)}\left[\sum_{u=i-(K-L)+1}^{K} a_u\right]}\right), \quad (47)$$

where $L \in (1, 2, ..., K)$ and we set the condition that $L > K - 1$.

3.3. Average Achievable Rate for V-VLC

For a V-VLC system, the average achievable rate at node R related with destination node D_1, denoted as $\mathcal{T}_{SR_1}^{VLC}$, can be expressed as,

$$\mathcal{T}_{SR_1}^{VLC} = \int_{v=0}^{\infty} \mathbb{P}\left[\frac{1}{2}\log_2\left(1 + \frac{e}{2\pi}\gamma_{SR_1}^{VLC}\right) > v\right] dv$$

$$= \int_{v=0}^{\frac{1}{2}\log_2(1+\frac{e}{2\pi}\frac{a_1}{a_2})} \mathbb{P}\left[\gamma_{SR_1}^{VLC} > \frac{2\pi}{e}(2^{2v} - 1)\right] dv$$

$$= \int_v \mathbb{P}\left[I_{VLC} < \frac{z(a_1 - \theta a_2)P_{VLC}d_0^{\frac{4}{\epsilon}}(H^2 + d_0^2)^{-(\frac{2\epsilon+2}{\epsilon})}}{\theta}\right] dv$$

$$= \int_v \mathcal{F}_{I_{VLC}}\left(\frac{z(a_1 - \theta a_2)P_{VLC}d_0^{\frac{4}{\epsilon}}(H^2 + d_0^2)^{-(\frac{2\epsilon+2}{\epsilon})}}{\theta}\right) dv, \quad (52)$$

where $\theta = \frac{2\pi}{e}(2^{2v} - 1)$ and $\mathcal{F}_{I_{VLC}}(\cdot)$ denotes the CDF of interference caused from V2V communication. This CDF expression can be expressed as [17],

$$\mathcal{F}_{I_{VLC}}(x) = \xi_c\left(\sqrt{\frac{\pi(\rho\lambda)^2 z}{4x}}\right), \quad (53)$$

where ξ_c is the complementary error function.

Similarly, the average achievable rate at node R associated with D_2 vehicle due to the V-VLC link, denoted as $\mathcal{T}_{SR_2}^{VLC}$, can be represented as,

$$\mathcal{T}_{SR_2}^{VLC} = \int_{v=0}^{\infty} \mathbb{P}\left[\frac{1}{2}\log_2\left(1 + \frac{e}{2\pi}\gamma_{SR_2}^{VLC}\right) > v\right] dv$$

$$= \int_v \mathcal{F}_{I_{VLC}}\left(\frac{za_2 P_{VLC}d_0^{\frac{4}{\epsilon}}(H^2 + d_0^2)^{-(\frac{2\epsilon+2}{\epsilon})}}{\theta}\right) dv. \quad (54)$$

The expression for average achievable rate at relay node R_i for K destination nodes can be given as [17],

$$\mathcal{T}_{SR_i}^{VLC} = \int_{v=0}^{v'} \mathcal{F}_{I_{VLC}}\left(\frac{z\left(a_i - \theta\left[\sum_{u=i+1}^{K} a_u\right]\right)}{\theta}\right.$$

$$\left. \times P_{VLC}d_0^{\frac{4}{\epsilon}}(H^2 + d_0^2)^{-(\frac{2\epsilon+2}{\epsilon})}\right) dv, \quad (55)$$

where $v' = \frac{1}{2}\log_2\left(1 + \frac{e}{2\pi}\frac{a_i}{\sum_{u=i+1}^{K} a_u}\right)$.

3.4. Average Achievable Rate for V-RF

For a V-RF system, the average achievable rate at relay node R associated with D_1 node, denoted as $\mathcal{T}_{SR_1}^{RF}$, can be expressed as [70],

$$\mathcal{T}_{SR_1}^{RF} = \frac{1}{2}\mathbb{E}[\log_2(1 + \gamma_{SR_1}^{RF})]$$

$$= \int_{v=0}^{\frac{1}{2}\log_2\left(1+\frac{a_1}{a_2}\right)} \mathcal{G}_R\left(\frac{2^{2v} - 1}{(a_1 + a_2 - a_2 2^{2v})P_{RF}l_{SR}}\right) dv. \quad (56)$$

Similarly, the average achievable rate at R associated with D_2 node due to the V-RF link, denoted as $\mathcal{T}_{SR_2}^{RF}$, can be given as,

$$\mathcal{T}_{SR_2}^{RF} = \frac{1}{2}\mathbb{E}[\log_2(1 + \gamma_{SR_2}^{RF})]$$

$$= \int_{v=0}^{\infty} \mathcal{G}_R\left(\frac{2^{2v} - 1}{a_2 P_{RF}l_{SR}}\right) dv. \quad (57)$$

The average achievable rate at R due to the combined effect of V-VLC and V-RF link associated with D_i message, where where i $\in \{1, 2\}$, can be expressed as[4],

$$\mathcal{T}_{SR_i} = \max(\mathcal{T}_{SR_i}^{VLC}, \mathcal{T}_{SR_i}^{RF}). \quad (58)$$

The average achievable rate at destination node D_1 when R broadcasts the message to D_1, denoted by $\mathcal{T}_{RD_1}$, can be given as,

$$\mathcal{T}_{RD_1} = \frac{1}{2}\mathbb{E}[\log_2(1 + \gamma_{RD_1})]$$

$$= \int_{v=0}^{\frac{1}{2}\log_2\left(1+\frac{a_1}{a_2}\right)} \mathcal{G}_{D_1}\left(\frac{2^{2v} - 1}{(a_1 + a_2 - a_2 2^{2v})P_{RF}l_{RD_1}}\right) dv. \quad (59)$$

---

[4]V-RF and V-VLC are two different vehicular technologies. For ease of analysis, we assume that average achievable rate evaluated at relay is maximum of average achievable rate associated with either V-VLC or V-RF link.

$$\mathcal{T}_{D_1} = \int_{v=0}^{\frac{1}{2}\log_2\left(1+\frac{a_1}{a_2}\right)} \frac{l_{RD_1}\mathcal{G}_{D_1}\left(\frac{2^{2v}-1}{(a_1-(2^{2v}-1)a_2)P_{RF}l_{RD_1}}\right) - l_{SD_1}\mathcal{G}_{D_1}\left(\frac{2^{2v}-1}{(a_1-(2^{2v}-1)a_2)P_{RF}l_{SD_1}}\right)}{l_{RD_1} - l_{SD_1}} dv. \tag{63}$$

The average achievable rate at node D_2 when R broadcasts the message to D_2, denoted by $\mathcal{T}_{RD_2}$, can be expressed as,

$$\mathcal{T}_{RD_2} = \frac{1}{2}\mathbb{E}[\log_2(1 + \gamma_{RD_2})]$$

$$= \int_{v=0}^{\infty} \mathcal{G}_{D_2}\left(\frac{2^{2v}-1}{a_2 P_{RF} l_{RD_2}}\right) dv. \tag{60}$$

The overall average achievable rate at vehicular node D_i due to hybrid transmission without MRC, can be expressed as,

$$\mathcal{T}_{D_i} = \min(\mathcal{T}_{RD_i}, \mathcal{T}_{SR_i}) \tag{61}$$

where $i \in \{1, 2\}$. After applying MRC, the average achievable rate associated with vehicular node D_1 is represented as [60],

$$\mathcal{T}_{D_1} = \frac{1}{2}\mathbb{E}[\log_2(1 + \gamma_{D_1})]. \tag{62}$$

On further solving the above equation, we obtain (63). Similarly, after applying MRC on D_2 node, the average achievable rate, is represented as,

$$\mathcal{T}_{D_2} = \frac{1}{2}\mathbb{E}[\log_2(1 + \gamma_{D_2})]$$

$$= \int_{v=0}^{\infty} \frac{l_{RD_2}\mathcal{G}_{D_2}\left(\frac{2^{2v}-1}{a_2 P_{RF} l_{RD_2}}\right) - l_{SD_2}\mathcal{G}_{D_2}\left(\frac{2^{2v}-1}{a_2 P_{RF} l_{SD_2}}\right)}{l_{RD_2} - l_{SD_2}} dv. \tag{64}$$

The overall average achievable rate at vehicular node D_i after applying MRC can be represented as,

$$\mathcal{T}_{D_i}^{MRC} = \min(\mathcal{T}_{R_i}, \mathcal{T}_{D_i}). \tag{65}$$

where $i \in \{1, 2\}$. The average achievable rate at relay node R_i for K destination nodes can be expressed as [70],

$$\mathcal{T}_{SR_i}^{RF} = \int_{v=0}^{v'} \mathcal{G}_R\left(\frac{2^{2v}-1}{\left(a_i - (2^{2v}-1)\left[\sum_{u=i+1}^{K} a_u\right]\right)P_{RF} l_{SR}}\right) dv. \tag{66}$$

Table 2
System Model Parameters

Parameter	Symbol	Value
Lambertian Order	m	1 [71]
Relay Position	R	(0,0)
Source Position	S	(-50,0)
Destination D_1 Position	D_1	(0,70)
Destination D_2 Position	D_2	(120,0)
Transmission power for VLC	P_{VLC}	33 dBm [17]
Optical Filter Gain	$T_s(\psi_k)$	1
Responsivity	$\mathcal{R}$	0.54 A/W [71]
Refractive Index	n	1
Photodiode Detection Area	A	$1cm^2$ [71]
Aperture Diameter	D_R	0.01m
Path Loss Exponent	α	2
Transmission power for RF	P_{RF}	23 dBm [17]
Height of Relay	H	8m

where $v' = \frac{1}{2}\log_2\left(1 + \frac{a_i}{\sum_{u=i+1}^{K} a_u}\right)$. The average achievable rate at node D_i due to $R \rightarrow D_i$ transmission, denoted as $\mathcal{T}_{RD_i}$, can be expressed as,

$$\mathcal{T}_{RD_i}$$

$$= \int_{v=0}^{v'} \mathcal{G}_{D_i}\left(\frac{2^{2v}-1}{\left(a_i - (2^{2v}-1)\left[\sum_{u=i+1}^{K} a_u\right]\right)P_{RF} l_{RD_i}}\right) dv. \tag{67}$$

After applying MRC at D_i [60], the average achievable rate, denoted by $\mathcal{T}_{D_i}$, is given by equation (68).

4. NUMERICAL RESULTS AND DISCUSSIONS

In this section, we present the results of our proposed framework for hybrid transmission with and without MRC. We also compare the results of a hyrbid V-VLC/V-RF system with a conventional V-RF system. The system model parameters for V-VLC and V-RF system are summarised in Table I. We assume the vehicular intensities at road X and Y to be the same, that is, $\lambda_X = \lambda_Y = \lambda$. As mentioned before, we consider different data requirements of each destination vehicular nodes, the target data rate of vehicular node D_2 is assumed

$$\mathcal{T}_{D_i} = \int_{v=0}^{v'} \frac{l_{RD_i}\mathcal{G}_{D_i}\left(\dfrac{2^{2v}-1}{\left(a_i-(2^{2v}-1)\left[\displaystyle\sum_{u=i+1}^{K}a_u\right]\right)P_{RF}l_{RD_i}}\right) - l_{SD_i}\mathcal{G}_{D_i}\left(\dfrac{2^{2v}-1}{\left(a_i-(2^{2v}-1)\left[\displaystyle\sum_{u=i+1}^{K}a_u\right]\right)P_{RF}l_{RD_i}}\right)}{l_{RD_i} - l_{SD_i}} dv. \qquad (68)$$
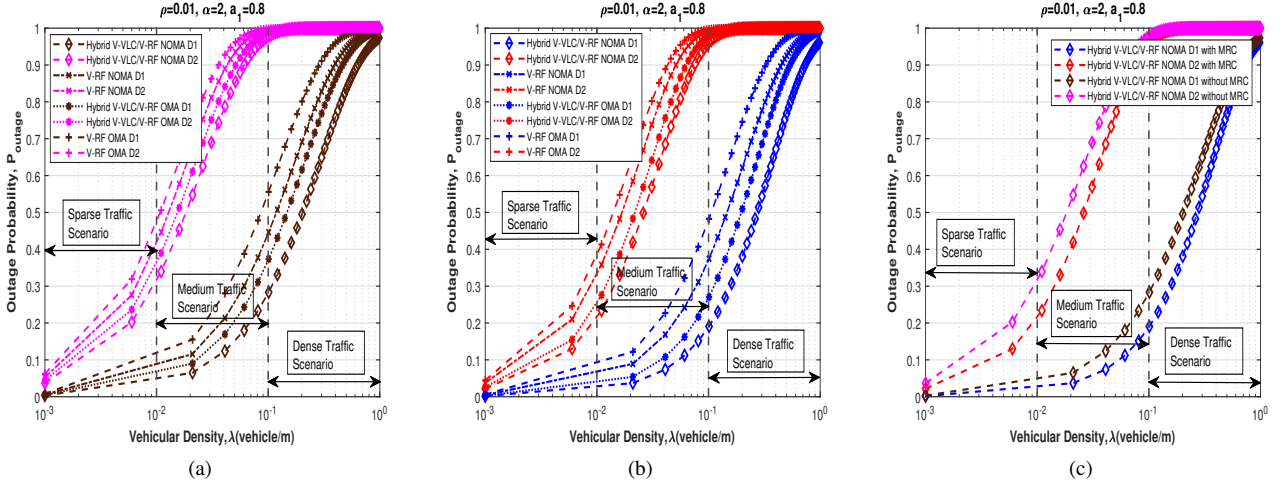

Figure 4: Outage probability as a function of vehicular density λ: (a) Hybrid transmission without MRC, (b) Hybrid transmission with MRC, and (c) Performance comparison for hybrid V-VLC/V-RF with and without MRC.

to be more than D_1 node. Monte Carlo simulations are performed to corroborate our theoretical equations. We have considered a worst case scenario when the interference from same lane or perpendicular lane vehicles are originating from an infinite road segment ($\mathcal{B} = \mathbb{R}^1$).

Fig. 4 illustrates the performance of outage probability for varying vehicular densities, λ. We observe that as the vehicular density increases, the outage probability associated with destination nodes D_1 and D_2 also increases. To observe the benefits of using a hybrid based system, we evaluate and compare the performance of hybrid V-VLC/V-RF based system with the conventional V-RF. From Fig. 4(a) we notice that, for a vehicular density of 0.01, outage probability associated with D_1 for a hybrid V-VLC/V-RF case is 0.05, while for V-RF case, it is approximately 0.12. Similarly, outage probability associated with D_2 for a hybrid V-VLC/V-RF is 0.32, while for V-RF case it is around 0.42. Fig. 4(b) represents hybrid transmission without MRC. For vehicular density, λ=0.01, outage probability associated with D_1 for a hybrid V-VLC/V-RF system is 0.03, whereas for a V-RF system it is approximately 1. Similarly, outage probability associated with D_2 for a hybrid V-VLC/V-RF system is 0.21 whereas for a V-RF system it is 0.34. The outage performance for hybrid transmission with and without MRC is better than a conventional V-RF system. Further, we also analyze the NOMA and OMA results for two user scenarios and observe that for both D_1 and D_2 destination vehicles, the outage performance of the NOMA overpowers that of OMA. Fig. 4(c) depicts the performance comparison

for a hybrid V-VLC/V-RF network scenario with and without MRC. We observe that irrespective of traffic scenario, the results for the MRC case have a better outage performance compared to the reception without MRC for both D_1 and D_2 vehicular nodes. For reception with MRC, D_1 and D_2 decode the coherently combined information received from both source node S and relay node R, thus increasing the received SIR at the vehicular nodes D_1 and D_2.

Fig. 5 depicts the the impact of varying power allocation coefficient on the outage probability. It is worth mentioning here that as intuitive, with increase in a_1, the outage probability associated with D_1 decreases, whereas the outage probability of D_2 increases. We observe that the hybrid V-VLC/V-RF link performs better than the conventional V-RF link. From Fig. 5(a), for D_1 vehicle, OMA outperforms NOMA when $a_1 \in [0.55, 0.6]$ for a hybrid V-VLC/V-RF system. This is because for lower values of a_1, lower power is assigned to vehicular node D_1 and more power is assigned to D_2 node, consequently increasing the interference and outage at D_1. For $a_1 \in [0.6, 0.85]$, NOMA performs better than OMA, this is because, more power is now assigned to vehicular node D_1. On the other hand, for D_2 vehicle, NOMA performs better than OMA for $a_1 \in [0.85, 1]$. Similarly, we observe from Fig. 5(b) that, for a hybrid V-VLC V-RF, OMA outperforms NOMA for $a_1 \in [0.55, 0.6]$. For D_2 vehicle, NOMA provides an enhanced performance over OMA for $a_1 \in [0.85, 1]$. In a hybrid V-VLC/V-VRF scenario, when $a_1 \in [0.6, 0.85]$, NOMA performs better than OMA for both D_1 and D_2 destination nodes. On
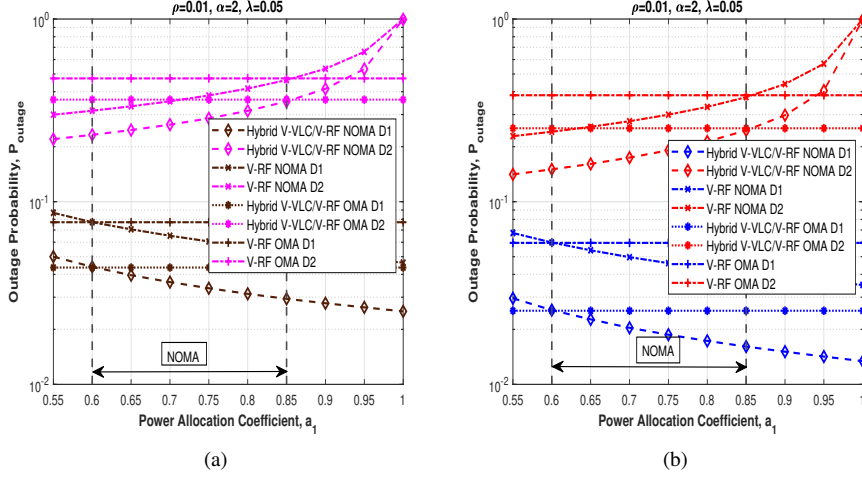
Figure 5: Outage probability as a function of power allocation coefficient a_1: (a) Hybrid transmission without MRC, (b) Hybrid transmission with MRC.
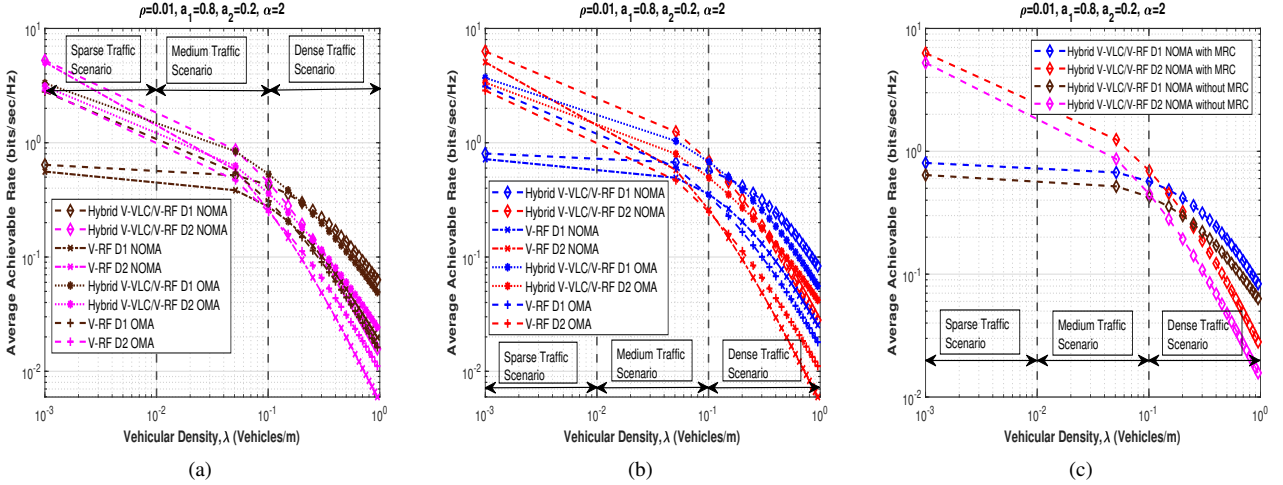

Figure 6: Average achievable rate as a function of vehicular density λ: (a) Hybrid transmission without MRC, (b) Hybrid transmission with MRC, and (c) Performance comparison for hybrid V-VLC/V-RF with and without MRC.

comparing Fig. 5(a) and 5(b), we note that the performance of a system using MRC reception is better than the system without MRC. For instance, with $a_1 = 0.8$, MRC reception has reduced the outage probability by 45% compared to the hybrid transmission without MRC.

Fig. 6 represents the performance of average achievable rate for varying vehicular densities, λ. For a sparse traffic and medium traffic scenario, vehicle D_1 has a lower achievable rate than vehicle D_2 because the D_2 vehicular node acts as an additional interference term for D_1 vehicle. As the vehicular density increases, D_1 vehicle provides a higher achievable rate than the vehicular node D_2. This is because, $a_1 > a_2$ and the effect of D_2 interference on D_1 becomes insignificant when compared to the other interfering vehicles on road X and Y. We also note that the performance of achievable rate in case of OMA for D_2 destination vehicle is more than the D_1 destination vehicle. Analysing Fig. 6(a)

for a hybrid V-VLC/V-RF scenario, vehicular node D_1 has a better performance of NOMA over OMA for $\lambda > 0.2$ vehicles/m. Similarly from Fig. 6(b), we observed that when $\lambda > 0.1$ vehicles/m, NOMA performs better than OMA in a hybrid V-VLC/V-RF scenario. Due to the directional property of VLC, the effect of interference on a hybrid V-VLC/V-RF system for a dense traffic scenario is significantly less than the conventional V-RF system. From Fig. 6(c), we observe that irrespective of traffic scenario, the achievable rate performance for a transmission with MRC is comparatively better than the system without MRC for a hybrid V-VLC/V-RF system.

In Fig. 7, we analyse the curves for average achievable rate for different power allocation coefficient a_1. For higher a_1, larger amount of power is assigned to node D_1, therefore we observe that, as the power allocation coefficient increases, the achievable rate associated with vehicular node
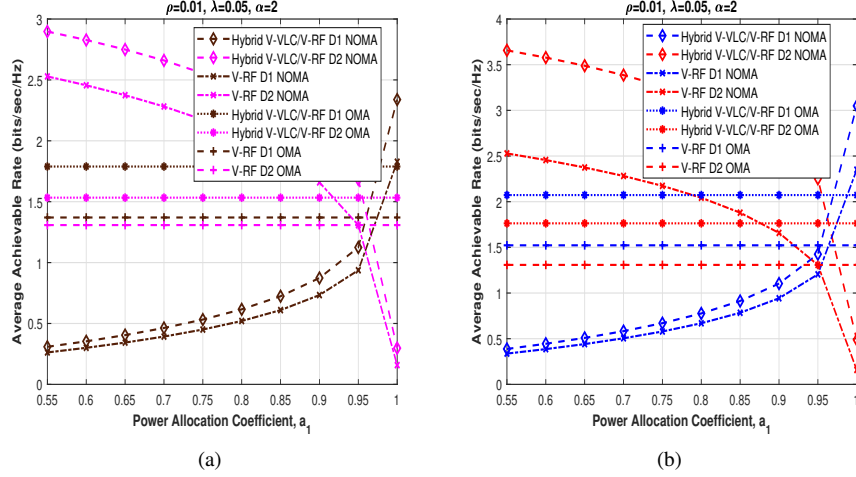
Figure 7: Average achievable rate as a function of power allocation coefficient a_1: (a) Hybrid transmission without MRC, (b) Hybrid transmission with MRC, and (c) Performance comparison for hybrid V-VLC/V-RF with and without MRC.
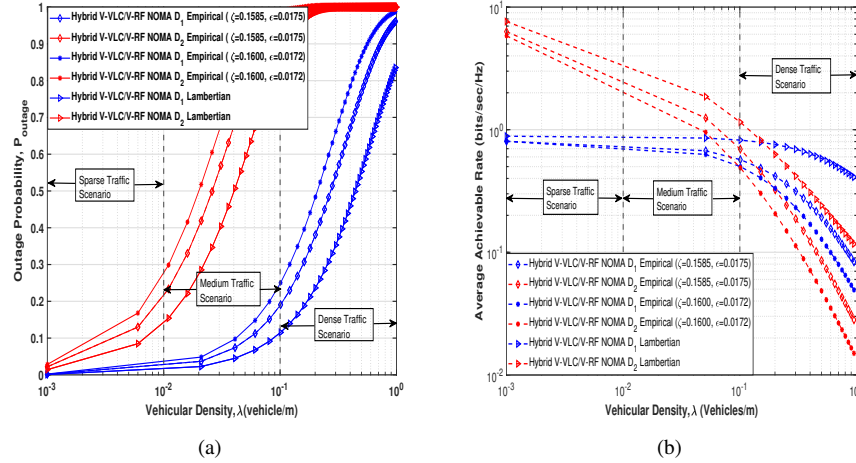

Figure 8: (a) Outage probability as a function of vehicular density λ for Lambertian and empirical model (b) Average achievable rate as a function of vehicular density λ for Lambertian and empirical model. Here, ρ=0.01, α=2 and a_1=0.8.

D_1 increases while that of the D_2 vehicle decreases. From Fig. 7(a), when $a_1 > 0.96$, NOMA has an enhanced performance compared to OMA for vehicular node D_1. Similarly for D_2 vehicle, NOMA performs better than OMA when $a_1 \in [0.55, 0.95]$. We also observe that for the D_2 vehicle, there is a noteworthy improvement in the average achievable rate for a hybrid V-VLC/V-RF based system compared to the conventional V-RF system. Similar analysis has been performed for Fig. 7(b). For D_2 destination vehicle, NOMA performs better than OMA when $a_1 \in [0.55, 0.97]$. Analyzing Fig. 7(a) and (b), we notice that on varying the power allocation coefficient, the hybrid transmission with MRC provides slightly better performance compared to the hybrid transmission without MRC. For MRC reception, when $a_1 > 0.98$, D_1 has a higher achievable rate than D_2 whereas for without MRC reception, D_1 has a better achievable rate performance when $a_1 > 0.96$.

Fig. 8(a) and (b) investigate the performance of an empirical model with respect to the Lambertian model in terms of outage performance and average achievable rate. It can be observed that Lambertian model has lower outage probability and high achievable rate as compared to the empirical model while employing the hybrid transmission with MRC. For $\lambda = 0.1$, the outage performance of the Lambertian model has decreased by 0.1 as compared to the empirical model. Similarly for D_2 destination vehicle, the outage performance of empirical model is 0.12 more than the Lambertian model. For dense traffic scenarios, Lambertian model offers higher achievable rate for both D_1 and D_2 destination vehicles as compared to the empirical VLC channel model. It has been observed that for $\lambda = 0.1$, the Lambertian model offers an achievable rate of 0.8 bits/s/Hz for D_1 node whereas the empirical model offers an average achievable rate of around 0.6 bits/s/Hz. It can be inferred from the above
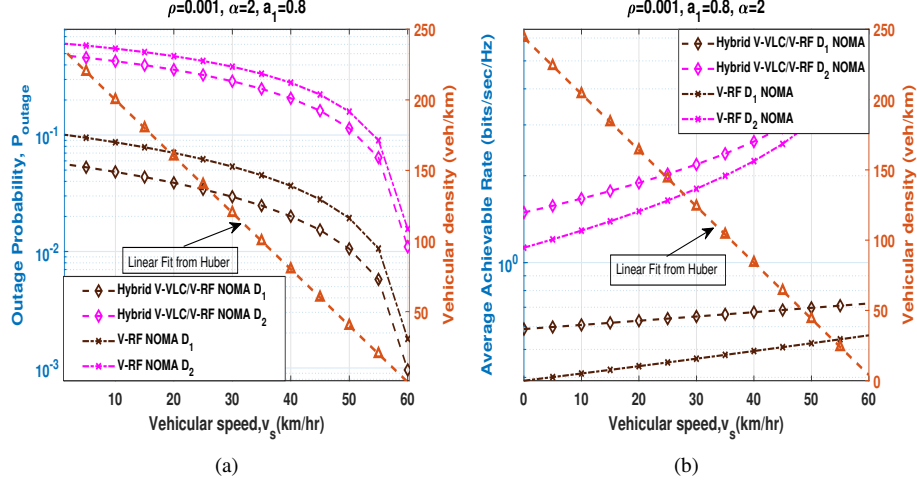
Figure 9: Impact of vehicular speed: (a) Outage probability, and (b) average achievable rate.
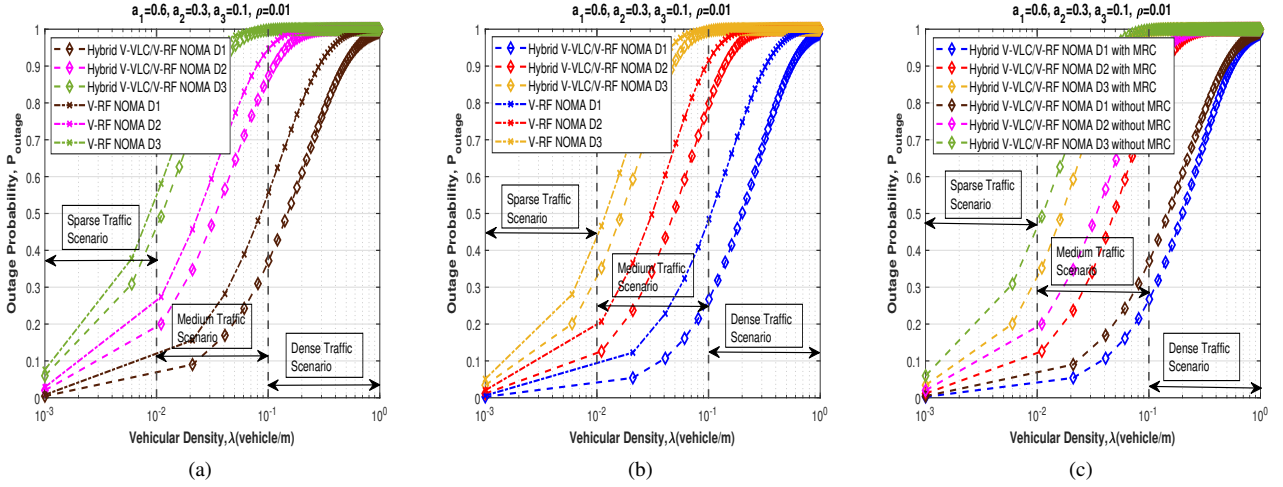

Figure 10: Outage performance as a function of vehicular density λ for $K = 3$ destination vehicles: (a) Hybrid transmission without MRC, (b) Hybrid transmission with MRC, and (c) Performance comparison for hybrid V-VLC/V-RF with and without MRC.

insights that given our simulation setting, empirical model is lower bound to the Lambertian model in terms of outage and average achievable rate performance. Next, we employ traffic flow theory (TFT[5])[6] to investigate the impact of vehicular speed, v_s[6]. Given the traffic flow $q = v_s \times \lambda$, we utilize speed-density flow model [72] to investigate the impact of v_s on the outage probability and average achievable rate. Fig. 9 illustrates the impact of vehicular speed on outage performance and average achievable rate for proposed C-NOMA supported V-VLC/V-RF scheme. Under stationary traffic condition, it can be observed that the outage and average rate improves with increase in vehicular speed. This

is due to fact that light traffic (low λ) supports high vehicular speed and vice versa obeying speed-density flow model. In more simpler words, in low traffic conditions, increasing the vehicle speed improves the outage and average achievable rate performance, whereas in high traffic conditions, decreasing the vehicle speed increases the performance.

For the sake of completeness, we analyze the performance of the network scenario for three destination vehicles with reference to outage probability and average achievable rate. The position of S, D_1, D_2, D_3 and R are (-50,0), (0,70), (120,0), (180,0) and (0,0) respectively. From Fig. 10(a) and 10(b), we observe and compare the outage performance of a hybrid V-VLC/V-RF based network scenario with a conventional V-RF system. As the vehicular density increases, we notice that the outage probability in a hybrid V-VLC/V-RF network scenario is less than a conventional V-RF system for all the three destination vehicles. The outage probability decreases by around 28% for D_3 destination node when

---

[5]TFT entails the knowledge of the fundamental characteristics of traffic flows (for instance, the road capacities, the relation between flow and density, and headway distributions) and the associated analytical methods[72].

[6]Shown under stationary traffic conditions, please note that under non-stationary traffic conditions, the time varying effects of V2X channels and Doppler shift are beyond the scope of this study and has been left as a subject of future investigation.
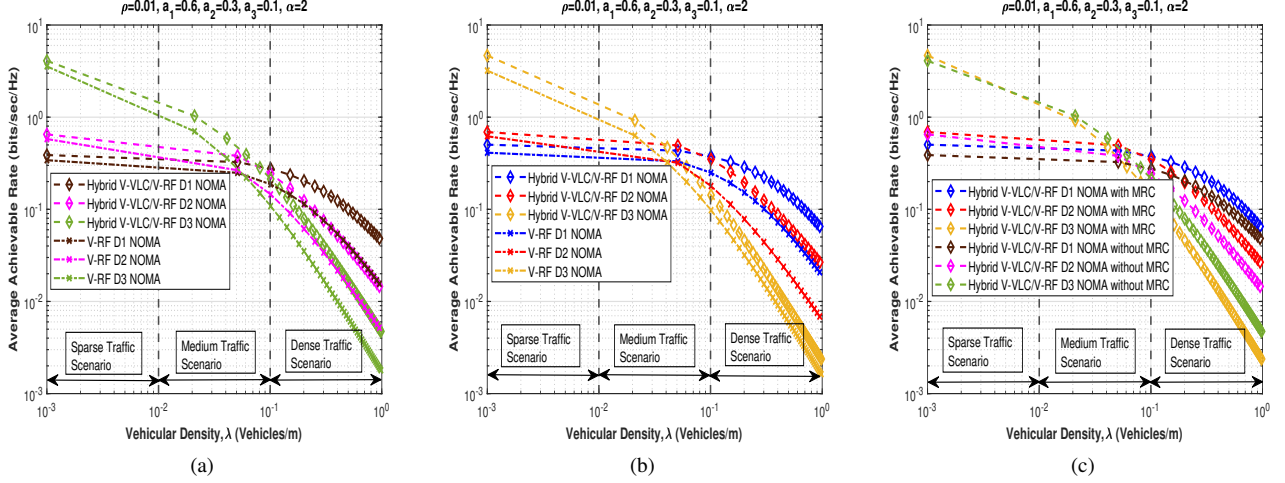
Figure 11: Average achievable rate as a function of vehicular density λ for $K = 3$ destination vehicles: (a) Hybrid transmission without MRC, (b) Hybrid transmission with MRC, and (c) Performance comparison for hybrid V-VLC/V-RF with and without MRC.

$\lambda = 0.01$. Fig 10(c) shows the comparison between hybrid transmission with and without MRC systems. We observe that the reception through MRC scheme outperforms the system transmitting without MRC. For a vehicular density of 0.01, D_3 vehicle has an outage of 0.32 for a MRC scenario whereas for without MRC case, the outage probability is 0.48. For the MRC case, vehicular nodes D_1, D_2 and D_3 decode the combined information received from both S and R, thus increasing the power at receiving nodes D_1, D_2 and D_3, and therefore increasing the overall SIR. Fig 11(a) and (b) analyse and compare the average achievable rate performance of a hybrid V-VLC/V-RF network with a conventional V-RF system. For a sparse traffic scenario, the performance of vehicular node D_3 with reference to achievable rate is better than the other vehicular nodes. This is because of the SIC that is performed at nodes D_1 and D_2, thus reducing the interference term at D_3 node. As the vehicular density increases, the average achievable rate of D_3 vehicle reduces drastically. Vehicular nodes D_1 and D_2 remain robust for dense traffic scenarios. The hybrid V-VLC/V-RF network provides an enhanced achievable rate over the conventional V-RF link for dense traffic scenario. Also, on analysing Fig. 11(c), we conclude that the performance of a hybrid transmission system with MRC is comparatively better than the hybrid transmission system without MRC.

5. CONCLUSION

In this paper, we explored the potential benefit of cooperative NOMA assisted hybrid V-VLC and V-RF solution to the V2X communication at road intersections. It has been shown through simulation results that the performance of the hybrid V-VLC/V-RF network is better than a conventional V-RF system in terms of outage probability and average achievable rate. The effectiveness of the proposed framework for the K destination vehicles scenario has been also

validated through results. We compared the performance of a hybrid transmission system with MRC over a hybrid transmission system without MRC and show that the MRC offers considerable improvement in terms of outage probability and average achievable rate. We also compared the performance of the Lambertian model with the empirical model and observed that the empirical model offers a higher outage and lower average achievable rate compared to the Lambertian model. We believe that this performance analysis of NOMA enabled hybrid V-VLC/V-RF network provides significant analytical contributions, while simulating new research direction as a future cooperative intelligent transportation system (C-ITS) alternative to meet diverse application needs for B5G V2X networks.

References

[1] World Health Organisation, *Road traffic injuries*, Jun. 2021. [Online]. Available: https://www.who.int/news-room/fact-sheets/detail/road-traffic-injuries.

[2] A. Afdhal and A. R. M. Shariff, "Traffic mobility analysis of its V2V cooperative awareness communication based on local traffic motion constraints," in *Proc. IEEE Int. Conf. on Cybernetics and Computational Intelligence*, 2019, pp. 120–125.

[3] M. Z. Chowdhury, M. T. Hossan, A. Islam, and Y. M. Jang, "A comparative survey of optical wireless technologies: Architectures and applications," *IEEE Access*, vol. 6, pp. 9819–9840, 2018.

[4] L. Cheng, W. Viriyasitavat, M. Boban, and H.-M. Tsai, "Comparison of radio frequency and visible light propagation channels for vehicular communications," *IEEE Access*, vol. 6, pp. 2634–2644, 2017.

[5] A.-M. Cailean, B. Cagneau, L. Chassagne, V. Popa, and M. Dimian, "A survey on the usage of DSRC and VLC in communication-based vehicle safety applications," in *Proc. IEEE 21st Symp. on Commun. and Veh. Technol. in the Benelux*, 2014, pp. 69–74.

[6] Y. Xiao, P. D. Diamantoulakis, Z. Fang, L. Hao, Z. Ma, and G. K. Karagiannidis, "Cooperative hybrid VLC/RF systems with SLIPT," *IEEE Trans. on Commun.*, vol. 69, no. 4, pp. 2532–2545, 2021.

[7] M. Noor-A-Rahim, Z. Liu, H. Lee, *et al.*, "6G for vehicle-to-everything (V2X) communications: Enabling technologies, challenges, and opportunities," *Proc. IEEE*, vol. 110, no. 6, pp. 712–734, 2022.

[8] H. Bagheri, M. Noor-A-Rahim, Z. Liu, *et al.*, "5G NR-V2X: Toward connected and cooperative autonomous driving," *IEEE Commun. Stand. Mag.*, vol. 5, no. 1, pp. 48–54, 2021.

[9] B. Di, L. Song, Y. Li, and Z. Han, "V2X meets NOMA: Non-orthogonal multiple access for 5G-enabled vehicular networks," *IEEE Wireless Commun.*, vol. 24, no. 6, pp. 14–21, 2017.

[10] İ. Coşandal, M. Koca, E. Biglieri, and H. Sari, "NOMA-2000 versus PD-NOMA: An outage probability comparison," *IEEE Commun. Lett.*, vol. 25, no. 2, pp. 427–431, 2020.

[11] R. C. Kizilirmak, C. R. Rowell, and M. Uysal, "Non-orthogonal multiple access (NOMA) for indoor visible light communications," in *Proc. IEEE 4th Int. Workshop Opt. Wireless. Commun.*, 2015, pp. 98–101.

[12] L. Yin, W. O. Popoola, X. Wu, and H. Haas, "Performance evaluation of non-orthogonal multiple access in visible light communication," *IEEE Trans. on Commun.*, vol. 64, no. 12, pp. 5162–5175, 2016.

[13] X. Guan, Q. Yang, Y. Hong, and C. C.-K. Chan, "Non-orthogonal multiple access with phase pre-distortion in visible light communication," *Opt. Exp.*, vol. 24, no. 22, pp. 25 816–25 823, 2016.

[14] Y. Fu, Y. Hong, L.-K. Chen, and C. W. Sung, "Enhanced power allocation for sum rate maximization in OFDM-NOMA VLC systems," *IEEE Photon. Technol. Lett.*, vol. 30, no. 13, pp. 1218–1221, 2018.

[15] C. Chen, W.-D. Zhong, H. Yang, and P. Du, "On the performance of MIMO-NOMA-based visible light communication systems," *IEEE Photon. Technol. Lett.*, vol. 30, no. 4, pp. 307–310, 2017.

[16] H. Marshoud, P. C. Sofotasios, S. Muhaidat, G. K. Karagiannidis, and B. S. Sharif, "Error performance of NOMA VLC systems," in *Proc. IEEE Int. Conf. on Commun.*, 2017, pp. 1–6.

[17] G. Singh, A. Srivastava, V. A. Bohara, and Z. Liu, "Downlink performance of optical power domain noma for beyond 5G enabled V2X networks," *IEEE Open J. Veh. Technol.*, 2021.

[18] G. Li and D. Mishra, "Cooperative noma networks: User cooperation or relay cooperation?" In *Proc. IEEE International Conference on Communications (ICC)*, 2020, pp. 1–6.

[19] L. Dai, B. Wang, Z. Ding, Z. Wang, S. Chen, and L. Hanzo, "A survey of non-orthogonal multiple access for 5G," *IEEE Commun. Surveys Tutorials*, vol. 20, no. 3, pp. 2294–2323, 2018.

[20] Z. Ding, M. Peng, and H. V. Poor, "Cooperative non-orthogonal multiple access in 5G systems," *IEEE Commun. Lett.*, vol. 19, no. 8, pp. 1462–1465, 2015.

[21] X. Liu, Y. Wang, and Z. Na, "Cooperative noma-based DCO-OFDM VLC system," in *International Conference on Green Communications and Networking*, Springer, 2019, pp. 14–24.

[22] Y. Xiao, P. D. Diamantoulakis, Z. Fang, Z. Ma, L. Hao, and G. K. Karagiannidis, "Hybrid lightwave/RF cooperative NOMA networks," *IEEE Trans. Wireless Commun.*, vol. 19, no. 2, pp. 1154–1166, 2020.

[23] S. I. Mushfique, P. Palathingal, Y. S. Eroglu, M. Yuksel, I. Guvenc, and N. Pala, "A Software-defined multi-element VLC architecture," *IEEE Commun. Mag.*, vol. 56, no. 2, pp. 196–203, 2018.

[24] H. Burchardt, N. Serafimovski, D. Tsonev, S. Videv, and H. Haas, "VLC: Beyond point-to-point communication," *IEEE Commun. Mag.*, vol. 52, no. 7, pp. 98–105, 2014.

[25] Z. Ghassemlooy, W. Popoola, and S. Rajbhandari, *Optical Wireless Communications: System and Channel Modelling with Matlab*. CRC Press, 2019.

[26] C. Tebruegge, A. Memedi, and F. Dressler, "Reduced multiuser-interference for vehicular VLC using SDMA and matrix headlights," in *Proc. IEEE Glob. Commun. Conf.*, 2019, pp. 1–6.

[27] A. Singh, G. Ghatak, A. Srivastava, V. A. Bohara, and A. K. Jagadeesan, "Performance analysis of indoor communication system using off-the-shelf LEDs with human blockages," *IEEE Open Journal of the Commun. Society*, vol. 2, pp. 187–198, 2021.

[28] J. Chen and Z. Wang, "Topology control in hybrid VLC/RF vehicular ad-hoc network," *IEEE Trans. on Wireless Commun.*, vol. 19, no. 3, pp. 1965–1976, 2019.

[29] N. Kumar, D. Terra, N. Lourenco, L. N. Alves, and R. L. Aguiar, "Visible light communication for intelligent transportation in road safety applications," in *Proc. IEEE 7th Int. Wireless Commun. and Mobile Computing Conf.*, 2011, pp. 1513–1518.

[30] H. Abuella, F. Miramirkhani, S. Ekin, M. Uysal, and S. Ahmed, "ViLDAR—visible light sensing-based speed estimation using vehicle headlamps," *IEEE Trans. on Veh. Technol.*, vol. 68, no. 11, pp. 10 406–10 417, 2019.

[31] F. M. Alsalami, N. Aigoro, A. A. Mahmoud, *et al.*, "Impact of vehicle headlights radiation pattern on dynamic vehicular VLC channel," *Journal of Lightwave Technol.*, vol. 39, no. 10, pp. 3162–3168, 2021.

[32] H. B. Eldeeb, E. Eso, E. A. Jarchlo, *et al.*, "Vehicular VLC: A ray tracing study based on measured radiation patterns of commercial taillights," *IEEE Photonics Technol. Lett.*, 2021.

[33] B. Aly, M. Elamassie, and M. Uysal, "Vehicular VLC channel model for a low-beam headlight transmitter," in *Proc. 17th Int. Symp. on Wireless Commun. Systems*, IEEE, 2021, pp. 1–5.

[34] M. Karbalayghareh, F. Miramirkhani, H. B. Eldeeb, R. C. Kizilirmak, S. M. Sait, and M. Uysal, "Channel modelling and performance limits of vehicular visible light communication systems," *IEEE Trans. on Veh. Technol.*, vol. 69, no. 7, pp. 6891–6901, 2020.

[35] T. Hardes and C. Sommer, "Towards heterogeneous communication strategies for urban platooning at intersections," in *Proc. IEEE Veh. Netw. Conf.*, 2019, pp. 1–8.

[36] H. Zhang, N. Liu, K. Long, J. Cheng, V. C. Leung, and L. Hanzo, "Energy efficient subchannel and power allocation for software-defined heterogeneous VLC and RF networks," *IEEE J. Selected Areas in Commun.*, vol. 36, no. 3, pp. 658–670, 2018.

[37] M. Kashef, M. Ismail, M. Abdallah, K. A. Qaraqe, and E. Serpedin, "Energy efficient resource allocation for mixed RF/VLC heterogeneous wireless networks," *IEEE J. Selected Areas in Commun.*, vol. 34, no. 4, pp. 883–893, 2016.

[38] T. Rakia, H.-C. Yang, F. Gebali, and M.-S. Alouini, "Optimal design of dual-hop VLC/RF communication system with energy harvesting," *IEEE Commun. Lett.*, vol. 20, no. 10, pp. 1979–1982, 2016.

[39] X. Bao, J. Dai, and X. Zhu, "Visible light communications heterogeneous network (VLC-HetNet): New model and protocols for mobile scenario," *Wireless Networks*, vol. 23, no. 1, pp. 299–309, 2017.

[40] Y. Xiao, P. D. Diamantoulakis, Z. Fang, Z. Ma, L. Hao, and G. K. Karagiannidis, "Hybrid lightwave/RF cooperative NOMA networks," *IEEE Trans. on Wireless Commun.*, vol. 19, no. 2, pp. 1154–1166, 2019.

[41] H. Tabassum and E. Hossain, "Coverage and rate analysis for co-existing RF/VLC downlink cellular networks," *IEEE Trans. on Wireless Commun.*, vol. 17, no. 4, pp. 2588–2601, 2018.

[42] J. Men and J. Ge, "Non-orthogonal multiple access for multiple-antenna relaying networks," *IEEE Commun. Lett.*, vol. 19, no. 10, pp. 1686–1689, 2015.

[43] M. Liaqat, K. A. Noordin, T. A. Latef, and K. Dimyati, "Power-domain non orthogonal multiple access (PD-NOMA) in cooperative networks: An overview," *Wireless Networks*, vol. 26, no. 1, pp. 181–203, 2020.

[44] Y. Saito, Y. Kishiyama, A. Benjebbour, T. Nakamura, A. Li, and K. Higuchi, "Non-orthogonal multiple access (NOMA) for cellular future radio access," in *Proc. IEEE 77th Veh. Technol. Conf.*, 2013, pp. 1–5.

[45] Z. Ding, Z. Yang, P. Fan, and H. V. Poor, "On the performance of non-orthogonal multiple access in 5G systems with randomly deployed users," *IEEE Signal Processing Lett.*, vol. 21, no. 12, pp. 1501–1505, 2014.

[46] X. Yue, Y. Liu, S. Kang, A. Nallanathan, and Z. Ding, "Exploiting full/half-duplex user relaying in NOMA systems," *IEEE Trans. Commun.*, vol. 66, no. 2, pp. 560–575, 2018.

[47] C. Zhong and Z. Zhang, "Non-orthogonal multiple access with cooperative full-duplex relaying," *IEEE Commun. Lett.*, vol. 20, no. 12, pp. 2478–2481, 2016.

[48] M. J. Farooq, H. ElSawy, and M.-S. Alouini, "A stochastic geometry model for multi-hop highway vehicular communication," *IEEE Trans. on Wireless Commun.*, vol. 15, no. 3, pp. 2276–2291, 2015.

[49] R. Tanbourgi, H. Jäkel, and F. K. Jondral, "Cooperative relaying in a poisson field of interferers: A diversity order analysis," in *Proc. IEEE Int. Symp. on Information Theory*, IEEE, 2013, pp. 3100–3104.

[50] S. N. Chiu, D. Stoyan, W. S. Kendall, and J. Mecke, *Stochastic Geometry and its Applications*. John Wiley & Sons, 2013.

[51] X. Gu, B. Leng, L. Zhang, J. Miao, and L. Zhang, "A stochastic geometry approach to model and analyze future vehicular communication networks," *IEEE Access*, vol. 8, pp. 14 500–14 512, 2020.

[52] M. N. Sial, Y. Deng, J. Ahmed, A. Nallanathan, and M. Dohler, "Stochastic geometry modeling of cellular V2X communication over shared channels," *IEEE Trans. on Veh. Technol.*, vol. 68, no. 12, pp. 11 873–11 887, 2019.

[53] E. Steinmetz, M. Wildemeersch, T. Q. Quek, and H. Wymeersch, "A stochastic geometry model for vehicular communication near intersections," in *Proc. IEEE Glob. Workshops*, 2015, pp. 1–6.

[54] Y. Sun and X. Dai, "Stochastic geometry based modeling and analysis on network NOMA in vehicular networks," in *Proc. IEEE Int. Conf. on Commun. Workshops*, 2020, pp. 1–6.

[55] T. Hou, Y. Liu, Z. Song, X. Sun, and Y. Chen, "Multiple antenna aided NOMA in UAV networks: A stochastic geometry approach," *IEEE Trans. on Commun.*, vol. 67, no. 2, pp. 1031–1044, 2018.

[56] S. Kusaladharma, W. Zhu, W. Ajib, and G. Amarasuriya, "Achievable rate analysis of NOMA in cell-free massive MIMO: A stochastic geometry approach," in *Proc. Int. Conf. on Commun.*, IEEE, 2019, pp. 1–6.

[57] S.-L. Wang and T.-M. Wu, "Stochastic geometric performance analyses for the cooperative NOMA with the full-duplex energy harvesting relaying," *IEEE Trans. on Vehicular Technol.*, vol. 68, no. 5, pp. 4894–4905, 2019.

[58] G. Singh, A. Srivastava, and V. A. Bohara, "Visible light and reconfigurable intelligent surfaces for beyond 5G V2X communication networks at road intersections," *IEEE Trans. Veh. Tech.*, pp. 1–1, 2022.

[59] G. Singh, A. Srivastava, V. A. Bohara, Z. Liu, M. Noor-A-Rahim, and G. Ghatak, "Heterogeneous visible light and radio communication for improving safety message dissemination at road intersection," *IEEE Trans. Intell. Transport. Syst.*, pp. 1–13, 2022.

[60] B. E. Y. Belmekki, A. Hamza, and B. Escrig, "Outage analysis of cooperative NOMA Using maximum ratio combining at intersections," in *Proc. IEEE Int. Conf. on Wireless and Mobile Computing, Netw. and Commun.*, 2019, pp. 1–6.

[61] M. Noor-A-Rahim, G. G. M. N. Ali, Y. L. Guan, B. Ayalew, P. H. J. Chong, and D. Pesch, "Broadcast performance analysis and improvements of the LTE-V2V autonomous mode at road intersection," *IEEE Trans. Veh. Tech.*, vol. 68, no. 10, pp. 9359–9369, 2019.

[62] Y. Yao, Z. Ni, W. Hu, and M. Motani, "Optimizing energy harvesting decode-and-forward relays with decoding energy costs and energy storage," *IEEE Access*, vol. 9, pp. 96 613–96 628, 2021.

[63] Z. Ding, Z. Yang, P. Fan, and H. V. Poor, "On the performance of non-orthogonal multiple access in 5G systems with randomly deployed users," *IEEE Signal Proc. Lett.*, vol. 21, no. 12, pp. 1501–1505, 2014.

[64] Z. Ding, H. Dai, and H. V. Poor, "Relay selection for cooperative NOMA," *IEEE Wireless Commun. Lett.*, vol. 5, no. 4, pp. 416–419, 2016.

[65] Z. Ding, L. Dai, and H. V. Poor, "MIMO-NOMA design for small packet transmission in the internet of things," *IEEE Access*, vol. 4, pp. 1393–1405, 2016.

[66] B. E. Y. Belmekki, A. Hamza, and B. Escrig, "Performance evaluation of adaptive cooperative NOMA protocol at road junctions," in *Proc. IEEE 91st veh. tech. conf. (VTC2020-spring)*, IEEE, 2020, pp. 1–6.

[67] A. Costanzo and V. Loscri, "Adaptive energy saving technique with saturation avoidance for outdoor VLC," in *Proc. IEEE 95th Veh. Tech. Conf.: (VTC2022-Spring)*, 2022, pp. 1–5.

[68] E. Steinmetz, M. Wildemeersch, T. Q. Quek, and H. Wymeersch, "Packet reception probabilities in vehicular communications close to intersections," *IEEE Trans. on Intell. Transp. Syst.*, vol. 22, no. 5, pp. 2823–2833, 2020.

[69] M. Haenggi, *Stochastic geometry for wireless networks*. Cambridge University Press, 2012.

[70] B. E. Y. Belmekki, A. Hamza, and B. Escrig, "On the performance of 5G non-orthogonal multiple access for vehicular communications at road intersections," *Veh. Commun.*, vol. 22, p. 100 202, 2020.

[71] P. Luo, Z. Ghassemlooy, H. Le Minh, E. Bentley, A. Burton, and X. Tang, "Fundamental analysis of a car to car visible light communication system," in *Proc. 9th Int. Symp. on Commun. Syst., Netw. Digit. Sign*, 2014, pp. 1011–1016.

[72] S. Hoogendoorn and V. Knoop, "Traffic flow theory and modelling," *The transport system and transport policy: an introduction*, vol. 2, pp. 125–159, 2013.